Remote Sensing-Based Estimation of Evapotranspiration for Irrigation Performance Assessment: Case of Koga Irrigation Project, Amahara Region, Ethiopia.

Gedamu Amare Bihonegn

A Thesis Submitted to

The department of Geomatics Engineering

School of Civil Engineering and Architecture

Presented in Partial Fulfillment of the Requirement for the Degree of Master's of Science in Geodesy and Geomatics Engineering

Office of Graduate Studies

Adama Science and Technology University

Adama

December, 2017

Remote Sensing – Based Estimation of Evapotranspiration for Irrigation Performance Assessment: Case of Koga Irrigation Project, Amahara Region, Ethiopia.

Gedamu Amare Bihonegn

Advisor: Dr Hasen Raja

A Thesis Submitted to

The department of Geomatics Engineering

School of Civil Engineering and Architecture

Presented in Partial Fulfillment of the Requirement for the Degree of Master's of Science in Geodesy and Geomatics Engineering

Office of Graduate Studies

Adama Science and Technology University

Adama

December, 2017

DECLARATION

I hereby declare that this MSc Thesis is my original work and has not been presented for a degree in any other university, and all sources of material used for this thesis have been duly acknowledged.

Name: ____

Signature: ____

This MSc Thesis has been submitted for examination with my approval as thesis advisor.

Name: ____

Signature: ____

Date of

APPROVAL SHEET

We, the undersigned, members of the Board of Examiners of the final open defense by Gedamu Amare Bihonegn have read and evaluated his/her thesis entitled **Remote Sensing Based Estimation of Evapotranspiration for Irrigation Performance Assessment at Koga Irrigation Project**" and examined the candidate. This is, therefore, to certify that the thesis has been accepted in partial fulfillment of the requirement of the Degree of Geodesy and Geomatics Engineering.

______________________	______________________	______________________
Chair Person	Signature	Date
______________________	______________________	______________________
Advisor	Signature	Date
______________________	______________________	______________________
External Examiner	Signature	Date
______________________	______________________	______________________
Internal Examiner	Signature	Date
______________________	______________________	______________________
Department	Chair Signature	Date
______________________	______________________	______________________
School Dean	Signature	Date
______________________	______________________	______________________
Postgraduate Dean	Signature	Date

ACKNOWLEDGEMENT

First and foremost it is my pleasure to thank Dr. Hasan Raja the principal supervisor of this thesis, for his profound continuous technical and scientific guidance, patience, motivation and enthusiasm. He guided me in all facets of my research from the proposal conception to the final write-up. I would like thanks to Mister Muhammed co-supervisor of this thesis, for his help and suggestions. I really appreciate for his constructive comments and provided input in this thesis.

Big thanks to my best friend Getachew Workineh for his profound continuous technical and scientific guidance, encouragement and reviewing of the whole thesis, and Dr Danile Tesfaw for his great amount of advice and encouragement and review the whole document.

I am very grateful to my best friend Getachew Bayable who has been helping me by data downloading, encouragement and reviewing of the thesis.

The success of this thesis would not have been possible without the financial support from the Haramaya University, which is gratefully acknowledged. Moreover I would like to extend my gratitude to the Adama Science and Technology University for providing funds for the field research. At the end I would like grateful thanks to my Mather Mulu Alemu and Father Amare Bihonegn and the whole Family for their help and encouragement.

Table of Contents

LIST OF FIGURES

LIST OF TABLES

LIST OF ACRONYMS

ASL	Atmospheric Boundary Layer
CSA	Central Statistical Agency
CWD	Cop Water Deficit
CWR	Crop Water Requirement
CWSI	Crop Water Stress Index
DF	Depleted Fraction
DN	Digital Number
E	Evaporation
EBBR	Energy Balance Bowen Ration
E_F	Evaporative Fraction
ESUN	Mean Solar Exo-atmospheric Irradiation
ET	Evapotranspiration
ETa	Actual Evapotranspiration
ETc	Crop Evapotranspiration
ETM	Enhanced Thematic Mapper
ETo	Reference Evapotranspiration
FAO	Food and Agricultural Organization
GIS	Geographic Information System
H	Sensible Heat Flux
IR	Irrigation Requirement

Kc	Crop Coefficient
LAI	Leaf Area Index
MoWR	Ministry of Water Resource
MSL	Mean sellable
NDVI	Normalized Differential Vegetation Index
NIR	Near Infrared
OCR	Overall Consumed Ratio
OLI	Operational Land Imagery
RET	Relative Evapotranspiration
RWS	Relative Water Supply
Rn	Net Surface Radiation Flux
SAVI	Soil Adjusted Vegetation Index
SEBAL	Surface Energy Balance Algorithm for Land
SEBI	Surface Energy Balance Index
SEBS	Surface Energy Balance System
S-SEBI	Simplified Surface Energy Balance Index
T	Transpiration
TIRS	Thermal Infrared Sensor
TM	Thematic Mapper
Ts	Surface Temperature
UNESCO	United Nations Educational, scientific and Cultural Organization

ABSTRACT

Evapotranspiration is one of the climate elements, which plays an important role in water balance and effects on the ecosystem of any region. Evapotranspiration was estimated from meteorological data using food and agricultural organization (FAO) method and using surface energy balance algorithm for land (SEBAL) algorithm from remote sensing data (LANDSAT8 images). The study was conducted at Koga Irrigation project which is located near to Bahir Dar in Mecha Werda. The main objective of this study is to estimate evapotranspiration (ET) for irrigation performance assessment using SEBAL algorithm, cropwat 8 model and the reliable performance indicators. The analysis is carried out using Landsat-8 (OLI/TIRS) data and reference weather parameters like temperature, rainfall, humidity, wind speed and sunshine. The models were prepared to calculate the values of surface radiance, surface reflectance, surface albedo, normalized vegetation index, leaf area index, surface emissivity, surface temperature, net radiation, soil heat flux, sensible heat flux, latent heat flux, which were consequently employed to calculate the daily evapotranspiration at the time of satellite over pass. Interestingly, the result of actual evapotranspiration estimated from SEBAL model in January, February, March, April and May was 0.778, 0.885, 1.01, o.997 and 1.01 respectively. The reference evapotranspiration estimated from FAO method at the time of satellite overpass in January, February, March, April and May was 2.98, 3.39, 3.87, 3.82 and 3.82 respectively. The total amount of crop water requirement and irrigation requirement of Maize were 611.8 and 597.9 respectively. The total amount of crop water requirement and irrigation requirement of Potato and Onion were equal which was 428.6 and 418.6 respectively. This clearly shows that different crops requires different amount of water and also total harvesting time also vary. The study also assessed the performance of Koga Irrigation project based on different irrigation performance indicators were estimated. The indicators were relative water supply, overall consumed ratio, depleted fraction, crop water deficit and relative evapotranspiration which have overall average estimated value of 1.85, 0.55, 0.07, 3.18 and 0.09 respectively. All indicators estimated above were out of the range by standards except crop water deficit that indicates the Koga Irrigation project is not well performed upon its final potential.

Keywords: Remote Sensing, GIS, Evapotranspiration, Cropwat, ERDAS, CWR and IR

CHAPTER ONE

1. INTRODUCTION

1.1. Background

The irrigation potential in Africa is estimated at more than 42.5 million ha, while only 13.4 million ha (31.5%) of water are managed. Since numerous African countries consider water and irrigation management as key factors to achieve their food security and to secure access to drinking-water, integrated water resources management and the development of small-scale irrigation are incorporated in various policies or legislative. Ethiopia is the second most heavily populated country in Africa and is the poorest in the world, ranked among the last out of 208 countries, with a per capita gross national income of USD in 2003. According to the Central Statistical Agency of Ethiopia (CSA, 2008), the total population in Ethiopia for 2007 was estimated 73,918,505 about 83.83 percent of which lives in the rural areas depending on subsistence agriculture. Though agriculture is the dominant sector, most of Ethiopia's cultivated land is under rain-fed agriculture. Due to lack of water storage and large spatial and temporal variations in rainfall, there is no enough water for most farmers to harvest more than one time per year and hence there are frequent crop failures and droughts which have results food shortage currently facing the country (Awulachew, 2005). Irrigation is an old practice for crop production in arid and semi-arid regions where annual evapotranspiration exceeds precipitation. However, due to population pressure, increased demand for food and fiber, irrigation is becoming increasingly important in cool and humid region (Bastiaanssen, 2000).

In Ethiopia, irrigation was an age-old practice and continued to date with minimal scientific input in most parts of the country. The problems of land degradation, population pressure, low productivity in agriculture, improper utilization of resources, poor infrastructure, absence or poor level of adoption of technological innovations, etc., contribute for food insecurity in the country. The situation in the Amhara National Regional State as well as in Koga Irrigation Project is not different from the national situation.

Irrigation is practiced in Ethiopia since ancient times producing subsistence food crops. Irrigation activities started in the 1950s with principally large-scale projects for agricultural purposes and power generation (Dessalegn, 1999). Ethiopia has an area of 2,700,000ha potential irrigation areas. Today only 11% (289,530 ha) of the potential irrigation area is utilized. The Ethiopian highland is the source of the Abay, Awash, Tekeze, Mereb, Baro-Akobo and Omo rivers that flow to the west and southwest.

The need to monitor ET at a regional scale is becoming realized as an important matter in studies of global change. As Ayoub (2008) mentioned remote sensing is the only method for effectively and economically estimating ET from a wide area with spatial variation. Methods using Satellite remote sensing data (VIS, NIR, and TIR bands) to derive local, regional and global estimation of turbulent fluxes are a recent development. Among others Surface Energy Balance Algorithm for Land (SEBAL), Two-Source Energy Balance algorithm (TSEB), Surface Energy Balance Index (S-SEBI), Soil Energy Balance System (SEBS) are the most common ones. Among the current satellite remote sensing models, the SEBAL has been designed to calculate the energy portioning at the regional scale with minimum ground data.

SEBAL uses digital imagery data collected by a remote-sensing satellite measuring visible, near infrared and thermal infrared radiation. In the SEBLA model, ET is computed from satellite images and weather data using the surface energy balance. Since the satellite image provides information for the overpass time only, SEBLA computes an instantaneous ET flux for the image time. The ET flux is calculated for each pixel of the image as a “residual” of the surface energy budget equation. The principles and steps needed to apply SEBS to estimate evapotranspiration are described in Bastiaanssen (1995), Bastiaanssen (2003). Accurate estimation of Evapotranspiration (ET) using remote sensing and GIS techniques requires understanding effects of the input parameters to the model and used satellite data on the accuracy of the results.

Bastiaanssen, W. (2005) described the key principles of the SEBAL model and summarized its accuracy under several climatic conditions at both field and catchment scales over more than 30 countries around the world. Likewise, according to Zhang, X. (2008) studies the effects of surface heterogeneity on performance of SEBAL modeling. Zhang, X. suggested that landscape heterogeneity influence the remotely sensed predictions of heat fluxes. In addition, to the effect of landscape heterogeneity he also investigated the sensitivity of the SEBAL model parameters for mapping winter wheat ET. Based on the fact that the SEBAL model works well only for areas where sunny days dominate and with a relatively pollution-free atmosphere. The SEBAL model is highly sensitive to the sunshine duration parameters and a modification of SEBAL model important to improve the results of temporal interpolation.

The major advantages of SEBAL for the estimation of land surface fluxes from thermal remote sensing data was required minimum ground-based data, automatic internal correction, which prevents strict correction of atmospheric effects on surface temperature, internal calibration, which is done within each analyzed image. Besides its several advantages, it has several drawbacks as well. Major disadvantages of this method are Subjective specifications of representative hot/dry and wet/cool pixels within the image are required to determine model parameters a and b. it is not considered heterogeneous landscape mountainous regions. Due to this some adjustments are required based on a digital elevation model for Ts and u to account for the lapse rate. Estimated H is greatly affected by the errors in surface-air temperature differences or surface temperatures measurements and ignoring the effect of radiometer viewing angle, can cause variation in Ts by several degrees for some images. But selected study area was Koga irrigation project which has a homogenous landscape and we can apply SEBAL model to estimate actual evapotranspiration on this area.

1.2. Statement of the Problem

The challenges in the encouragement of irrigation development are not easy in the area as well as in other parts of the Amhara Region. The nature of farmland distribution is uneven and fragmented on the potentially irrigated lands (Molla, 2009). Some farmers do not manage their piece of land properly with the requirement of the irrigation system. These require accurate determination of Remote Sensing based, water requirement of each crop on each fragmented farmland for appropriate water supply. Performance gap in the area, the variation of the actual performance of irrigation from the target level, is the indicator of low performance. To increase the agricultural productivity by improving the management of the available resources, the national goals are developed. According to the MoWR (2002), different information from different stakeholders like irrigation managers at different levels (from high level irrigation experts up to DAs) have tried to identify the irrigation performance gaps, find the causes for the gap, and take corrective measures to cure the target performance (Dessalegn, 1999). But, this is not support by remote sensing based estimation of evapotranspiration. Evapotranspiration estimated from metrological data has a lot of drawbacks like it takes more time, cost, the data is not uniform and reliable as compared to remote sensing. Remote sensing solves the above drawback. Over the past period, significant changes at global and regional level have been observed in irrigation performance due to the unbalance of ET and water supply in the field. Under such conditions, more attention has been paid for irrigation performance related studies. However, little has been done to understand the interaction between ET, CWR and irrigation performance. Measuring evapotranspiration has great importance for understanding and manages the water cycle of irrigated areas and their field crops. Determining crop water requirement of individual crops are important for crop yield maximization.

Performance assessment done using remote sensing provides relevant feedback controls to the management, whereas performance indicators provide necessary information for those controls. In order to make decisions at the right time, the delays of acquiring and processing of field data should be minimized. So, remote sensing provides a potential capability for routinely monitoring ET at irrigated areas by combining remotely sensed data and ground meteorological data in a SEBAL model. This provides appropriate supply of irrigation water for the field based on the water requirement of the crop by balancing evapotranspiration of crops and crop water requirement.

1.3. Objective of the Study

1.3.1. General Objective

The main objective of the research was to estimate evapotranspiration for irrigation performance assessment using remote sensing data based on best combination of performance indicators.

1.3.2. Specific Objective

The specific objectives of the Study were:

- To estimate the spatial variation of actual evapotranspiration of Koga Irrigation Project using SEBAL algorithm and Penman-Monteith (FAO) Method.
- To determine crop water requirement and Irrigation schedules of major crops of Koga Irrigation Project.
- To assess the performance of Koga Irrigation Project using the appropriate performance indicators.

1.4. Research Questions

- What is the estimated spatial variation of evapotranspiration using SEBAL algorithm in the study area?
- How much is irrigation water requirements of major crops in the study area?
- Is performance of Koga Irrigation Project meet FAO's irrigation performance standards?

1.5. Scope of the study

The research focuses on Koga Irrigation project which was found in Merawi Werda, Amahara Region. This study focuses on estimation of evapotranspiration, crop water requirement and irrigation performance indicators estimated from satellite images (LANDSAT) and metrological data for irrigation performance assessment at Koga Irrigation. This study used both SEBAL model and FAO methods. In the computation of actual evapotranspiration NDVI, SAVI, LAI, surface temperature, albedo, emissivity, incoming short wave radiation, incoming long wave radiation, outgoing long wave radiation, net surface radiation flux, soil heat flux and sensible heat flux was estimated based on SEBAL model using ERDAS model maker. The reference evapotranspiration, crop water requirement, irrigation water requirement and irrigation schedules of major crops in the area was computed based on FAO method using cropwat 8 from weather data.

There are different indicators for irrigation performance assessments which is depends on the factors that affect the irrigation performance. Due to this, indicators like overall consumed ratio (OCR), relative water supply (RWS), depleted fraction (DF), crop water deficit (CWD) and relative evapotranspiration (RET) which was related to the environmental factors was used as indicator to measure the performance of irrigation rather than physical factors.

1.6. Significance of the study

The performance of irrigation can be reduced by different factors such as climate change, poor management system and lack of knowledge and skill of farmers. The low irrigation performance reduce productivity and difficult to prevent the residence from poverty. So, in this study the performance of irrigation is estimated and gives solution for the irrigation experts, community (stakeholders) and policy makers to solve the problem and increase productivity. The experts and farmers also know the amount of water required by crop and adjust it to encourage irrigation performance.

1.7. Organization of the Thesis

The report was organized into five chapters. The first chapter is an introduction part includes background, statement of the problem, objectives of the study, significance and scope of the study. The second chapter is literature reviews, which includes basic concepts of evapotranspiration, evaporation, transpiration, crop evapotranspiration, and crop and irrigation water requirement, different surface energy balance algorithms including SEBAL and irrigation performance indicators. The third chapter is focused on description of the study area (location and climate characteristics), data and data source, materials and methodology of the study which includes detail description of procedure of estimating evapotranspiration using ERDAS imagine model maker based on SEBAL, estimation of reference evapotranspiration, effective rainfall and crop water requirements and irrigation schedules from weather data using cropwat 8.0. The fourth chapter deals with result and discussion justified in detail. The last part chapter five is conclusion and recommendation.

CHAPTER TWO

2. LITERATURE REVIEW

2.1. Remote Sensing and Surface Energy Balance Algorithm for Land (SEBAL)

The potentiality of remote sensing techniques in irrigation and water resource management has been widely recognized. Environmental physics based on electromagnetic radiation and micro-hydrology has evolved in the development of quantitative algorithms to convert remotely sensed spectral radiances into useful information such as evapotranspiration, root zone soil moisture, and biomass growth. Estimation of crop water parameters using remote sensing techniques is an expanding research field and development trends have been progressing since 1970s (Bandara, 2006). The remote sensing algorithm such as SEBAL (Surface Energy Balance algorithm for land) was originally developed in the Netherlands for use in Egypt by Bastiaanssen and Chandrapala (1995) and was modified during the Idaho study for application to mountainous terrain and clear, Cold Lakes.

SEBAL modified by Bastiaanssen (2003) is currently used approaches to estimate crop water parameters. The scale of satellite measurements is a measure of its quality and which is associated with two parameters, namely spatial resolution and temporal resolution. The spatial resolution measures the ability of a sensor to distinguish among closely spaced objects in the terrain. One pixel is the smallest area of the terrain that can be recorded as a unique element by the sensor.

Calculation of water consumptions by remote sensing has been under high research efforts for the last 20 years, especially the energy balance models. Some dedicated energy-balance models like the SEBAL (Bastiaanssen, 1995) and also some related models calculating evapotranspiration are also available among others not mentioned here. To add to this non-extensive list, a lot of Global Climatologic Models use the energy-balance process for various outputs like ET or soil moisture. Typically, for crop ET monitoring, high spatial resolution satellites are required, but the list is restricted to satellites having the capacity to calculate the surface temperature, as the latent heat flux of vaporization is temperature driven. Some coarser spatial resolution satellites up to 1 Km pixel size are still used for irrigation system temporal ET monitoring. Larger spatial resolution satellites, generally for meteorological purposes, even if used largely in GCMs, are not used for crop monitoring. SEBLA is one of the thermodynamically based models available, which partitions the sensible heat flux and the latent heat flux of vaporization. The remote sensing technology application is under the expectation in Ethiopia, but it has rarely been applied to support irrigation management practices because of the associated costs and quality of images.

2.2. Evapotranspiration Concepts

Evapotranspiration (ET) is the loss of water to the atmosphere by the combined processes of evaporation from the soil and plant surface and transpiration from plants (Othoman, Clariza, Kenji, & Atsushi, 2006). Estimation of evapotranspiration is one of the major hydrological components for determining the water budget and is becoming essential for the calculation of a reliable recharge and evaporation rate for the groundwater flow analysis. It is therefore, reliable and consistent estimate of evapotranspiration is a great importance for the management of water resources efficiently.

In a cropped field water can be lost through two processes. The first process is Water can be lost from the soil surface and wet vegetation through a process called evaporation (E), whereby liquid water is converted into water vapor and removed from the evaporating surface. Energy is required to change the state of the molecules of water from liquid to vapor. The process is affected by climatological factors such as solar radiation, air temperature, air humidity and wind speed. Where the evaporating surface is the soil surface, the degree of shading of the crop canopy and the amount of water available at the evaporating surface are the other factors that affect the evaporation process. The second process of water loss is called transpiration (T), whereby liquid water contained in plant tissues vaporizes into the atmosphere through small openings in the plant leaf, called stomata (Andreas & Karen, 2002). Transpiration, like direct evaporation, depends on the energy supply, vapor pressure gradient and wind. Hence solar radiation, air temperature, air humidity and wind terms should be considered when assessing transpiration. The soil water content and the ability of the soil to conduct water to the roots also determine the transpiration rate, as do water logging and soil salinity. Crop characteristics, environmental aspects and cultivation practices also have an influence on the transpiration.

The combination of these two separate processes where by water is lost on one hand by evaporation from the soil surface and on the other hand by transpiration from a plant, is called evapotranspiration (ET). Evaporation and transpiration occur simultaneously and there is no easy way of distinguishing between the two processes.

2.2.1. Reference Crop Evapotranspiration

The evapotranspiration from a reference surface not short of water is called the reference crop evapotranspiration and is denoted by ETo. The reference surface is a hypothetical grass reference crop with specific characteristics. The concept of ETo was introduced to study the evaporative demand of the atmosphere independently of crop type, crop development stage and management practices. As water is abundant at the evapotranspiration surface, soil factors do not affect evapotranspiration. Relating evapotranspiration to a specific surface provides a reference to which evapotranspiration from other surfaces can be related. It removes the need to define a separate evapotranspiration level for each crop and stage of growth.

The only factors affecting ETo are climatic parameters. As a result, ETo is a climatic parameter and can be compute from weather data. ETo expresses the evaporative demand of the atmosphere at a specific location and time of the year and does not consider crop and soil factors.

2.2.2. Potential Evapotranspiration

Potential evapotranspiration of a particular crop refers to the reference evaporation adjusted to the characteristics of the crop (Perry *et al*, 2009). The characteristics of the crop are defined by the Kc factor as presented in Allen *et al*. (1998) for each crops. Potential evapotranspiration defines as the maximum amount of water that a specific crop can evaporate under the accessible environment with no limitations in water supply.

2.2.3. Actual Evapotranspiration

Actual evaporation is defined as the actual amount of water that lost to the atmosphere from vegetated surface. According to Perry *et al* (2009), under condition of full water supply like fully irrigated surface or during wet seasons the amount of actual evapotranspiration is equal to the potential evapotranspiration.

Actual evapotranspiration from remote sensing can be estimated from either the thermal or visible and NIR bands of the remote sensing images. In visible or NIR remote sensing, indicators such as normalized difference vegetation index (NDVI) are used together with crop coefficients (Kc) to obtain crop evapotranspiration (Akdim *et al*, 2014). In thermal remote sensing, land surface temperature is derived and used in energy balance model to estimate net surface radiation flux used as input to estimate actual evapotranspiration.

2.2.4. Crop Evapotranspiration, Crop Water and Irrigation Water Requirement

The crop evapotranspiration, denoted as ETc, is the evapotranspiration from disease-free and well-fertilized crops grown in large fields under optimum soil water conditions and achieving full production under the given climatic conditions. The values of ETc and CWR (Crop Water Requirements) are identical, whereby ETc refers to the amount of water lost through evapotranspiration and CWR refers to the amount of water that is needed to compensate for the loss (Andreas & Karen, 2002).

Irrigation requirements (IR) refer to the water that must be supplied through the irrigation system to ensure that the crop receives its full crop water requirements. If irrigation is the sole source of water supply for the plant, the irrigation requirement will always be greater than the crop water requirement to allow for inefficiencies in the irrigation system. If the crop receives some of its water from other sources (rainfall, water stored in the ground, underground seepage, etc.), then the irrigation requirement can be considerably less than the crop water requirement.

2.3. Factors Affecting Crop Evapotranspiration

The main factors affecting evapotranspiration are climatic parameters, crop characteristics, management practices and environmental aspects. The main climatic factors affecting evapotranspiration are solar radiation, air temperature, air humidity and wind speed. The crop type, variety and development stages affect evapotranspiration. Differences in crop resistance to transpiration, crop height, crop roughness, reflection, canopy cover and crop rooting characteristics result in different evapotranspiration levels in different types of crops under identical environmental conditions.

2.4. Different Surface Energy Balance Algorithms

2.4.1. Surface Energy Balance Index (SEBI)

SEBI estimated based on the contrast between dry and wet regions. Menenti and Choudhury (2013) proposed the Surface Energy Balance Index (SEBI) method to derive the evapotranspiration from evaporative fraction. This method is based on the Crop Water Stress Index (CWSI). In this approach, relative evaporation is determined by scaling an observed surface temperature in a maximum range of surface temperature, denoted by extremes in the surface energy balance suggesting a theoretical lower and upper bounds on the surface and air temperature difference. Here under dry-condition, evaporation is assumed to be zero due to the limitation of water availability in soil for a particular set of boundary layer characteristics so that the sensible heat flux density takes its maximum value Ts, max (maximum surface temperature).

2.4.2. Surface Energy Balance System (SEBS)

Another well-known model is the Surface Energy Balance System (SEBS). Su *et al*. (2002) described a modified form of SEBI for the estimation of land surface energy balance using remotely sensed data, which has been named SEBS. SEBS estimates sensible and latent heat fluxes from satellite data and routinely available meteorological data. Computations of land surface physical parameters, calculation of roughness length for heat transfer, and estimation of the evaporative fraction based on energy balance at limiting cases are the main bases of SEBS.

In SEBS, the latent heat flux is considered to be zero at the dry limit, which means sensible heat flux reaches its maximum value (i.e., Hdry = Rn − G). On the other hand, at the wet limit, ET takes place at potential rate (LEwet), (i.e., the evaporation is restricted only by the energy available for a particular surface and atmospheric condition) and the sensible heat flux attains its minimum value, Hwet. The sensible heat flux at dry and wet limits can be expressed as:

$$\mathrm{H_{dry}} = \mathrm{R_n} - \mathrm{G} \quad \ldots\ldots 1$$

By utilizing similarity theory, a distinction is made in SEBS between the Atmospheric Boundary Layer (ABL) and the Atmospheric Surface Layer (ASL). Such distinction is made to take the ABL height as a reference of potential air temperature to calculate the heat fluxes. Here a distinction is made between surface temperature and potential air temperature. Remote sensing data-derived land parameters and ground-based meteorological measurements are used as inputs in SEBS. Using remote sensing data from ATSR and ground data from a Numerical Weather Prediction model, Jia *et al* (2003) proposed a modified version of SEBS and validated the estimated sensible heat flux with large aperture scintillaometers. Wood *et al.* (1982) applied SEBS to the Southern Great Plains region of the United States and compared the latent heat fluxes with the measurements from the Energy Balance Bowen Ration (EBBR) sites. Their results indicate the potential usefulness of SEBS approach in estimating surface heat flux from space for data assimilation purposes. Daily, monthly, and annual estimation of evaporation in a semi-arid environment have been done by SEBS. SEBS can be even used for both local scaling and regional scaling under all atmospheric stability regimes as shown by Su *et al*. (2002) accuracy of ET value estimated from SEBS could reach 10%–15% of that of in-situ measurements even when evaporative fraction ranged from 0.5 to 0.9.

Main advantages of the SEBS include: (1) consideration of the energy balance at the limiting cases, which minimizes the uncertainty involved in surface temperature or meteorological variables; (2) new formulation of the roughness height for heat transfer instead of using constant values; (3) characterizing actual turbulent heat fluxes without any prior knowledge; and (4) representativeness of parameters associated with surface resistance.

Note that SEBS has been widely applied over large heterogeneous areas fed with MODIS data with thermal band information of 1 km. However, relatively complex solution of the turbulent heat fluxes and too many required parameters can often cause more or less inconveniences in SEBS when data are not readily available.

2.4.3. Simplified Surface Energy Balance Index (S-SEBI)

A simplified new method derived from SEBI, called Simplified Surface Energy Balance Index (S-SEBI), has been developed to estimate the surface flux from remote sensing data. Contrast between a reflectance (albedo) dependent maximum and minimum surface temperature for dry and wet conditions, respectively, is a main base of this method to partition available energy into sensible and latent heat fluxes. No additional meteorological data is needed if the surface extremes are available on the scene studied. By assuming stable global radiation and air temperature, a physical explanation to the observed surface reflectance and temperature in the S-

SEBI approach can be given when surface characteristics within the observed image changes between dark/wet and dry/bright pixels. At low reflectance, surface temperature remains almost constant with increasing reflectance because of the presence of sufficient water under these conditions. At higher reflectance, surface temperature increases to some value with the increase of reflectance and is designated as “evaporation controlled” because of the fact that the change in temperature at this stage is solely controlled by the decrease of evaporation resulting from the less soil moisture availability. Beyond the inflexion of reflectance, the surface temperature declines with the increase of surface reflectance. At this point, soil moisture shrinks to such a level that evaporation cannot occur. Therefore, the available energy is completely utilized for surface heating. Thus, an increase in surface reflectance yields a net radiation decrease, which in turn produces less surface heating and the corresponding surface temperature, which is referred as “radiation controlled”. Here, evaporative fraction (EF) is constrained by the dry and wet regions and formulated by interpolating the reflection-dependent surface temperature between the reflection-dependent maximum and minimum surface temperatures as shown in Equation (2):

$$EF = \frac{(T_H - T_S)}{(T_H - T_{LE})} \quad \ldots\ldots 2$$

Where TH is the land surface temperature corresponding to dry condition and represents the minimum latent heat flux (LEdry = 0) and maximum sensible heat flux (Hdry = Rn − G), and TLE is the land surface temperature corresponding to wet condition and represents the maximum latent heat flux (LEwet = (Rn − G)) and minimum sensible heat flux (Hwet = 0) for a given surface reflectance.

The major advantages of S-SEBI are that (1) Additional ground-based measurement is not needed to derive the EF except the surface temperature and reflectance (albedo) derived from remote sensing data if the surface extremes are present in the remotely sensed imagery; and (2) Extreme temperatures for the wet and dry conditions vary with changing reflectance (albedo) values, but in other methods like SEBAL, a fixed temperature is determined for wet and dry conditions.

2.4.4. Surface Energy Balance Algorithm for Land (SEBAL)

Surface Energy Balance Algorithm for Land (SEBAL), an image-processing model for calculating evapotranspiration (ET) as a residual of the surface energy balance, was developed in the Netherlands by Bastiaanssen (2000). Within the most promising approaches currently available to estimate evapotranspiration, the SEBAL has been designed to calculate the energy balance components, at both local and regional scales with minimum ground data. This model is an intermediate approach using both empirical relationships and physical parameterization. It requires digital imagery data collected by any satellite sensor measuring visible, near-infrared, and thermal infrared radiation, Ts, NDVI, and albedo maps. Latent heat flux (λE) is estimated as a residual of the energy balance equation on a pixel-by-pixel basis. Net surface radiation (Rn) is computed from the balance of short and long wave radiation.

Soil heat flux (G) is calculated utilizing the equation proposed by Bastiaanssen (1998), which is applicable to all sorts of vegetation cover and soil type. Under several climatic conditions, this method has been verified at both field and catchment scales with typical accuracy at field scale being 85% and 95% at daily and seasonal scales, respectively, in more than 30 countries worldwide. The estimation of sensible heat flux (H) is required to obtain the parameters that will allow the computation of ET as a residual from the energy balance. In SEBAL, two reference air temperatures are taken. One being an air temperature located at height h1 close to the surface and the other at an upper height h2. To determine the value of dT for each pixel, SEBAL assumes the existence of a linear relationship between dT and the radiometric surface temperature Ts considering homogeneous metrological and surface conditions. SEBAL algorithm was developed by Bastiannssen *et al*. (1998) and has been applied to LANDSAT ETM+ and TM images in the present study, along with weather data to compute seasonal and annual evapotranspiration. SEBAL can be processed using a number of programs such as ERDAS Imagine, MATLAB, and Arc GIS. Arc GIS has been chosen was used for its least complicated procedural algorithms. Arc GIS is a geospatial software package and does not require a complicated mathematical modeling background. It allows manipulation, plotting of functions, data implementation of algorithms, creation of raster data sets in simple and understandable formats like tiff and img format.

Among all the models used in the present research SEBAL is most complex with more than 30 computational steps. LANDSAT data used in SEBAL algorithm is available monthly except for two monsoon months were cloud cover is more than 80%. SEBAL computes an instantaneous ET flux for the satellite over pass time. This instantaneous ET is then converted to daily and monthly ET by various computational steps in SEBAL. The ET flux is calculated for each pixel of the image as a “residual” of the surface energy budget equation.

The major advantages of SEBAL for the estimation of land surface fluxes from thermal remote sensing data are (1) minimum use of auxiliary ground-based data; (2) automatic internal correction, which prevents strict correction of atmospheric effects on surface temperature; and (3) internal calibration, which is done within each analyzed image. Besides its several advantages, it has several drawbacks as well. Major disadvantages of this method are that (1) Subjective specifications of representative hot/dry and wet/cool pixels within the image are required to determine model parameters a and b. The resulting H flux and ET estimates from SEBAL can vary with differing extreme pixels selected by the operator, domain size, and spatial resolution of satellite sensors; (2) Over mountainous regions, some adjustments are required based on a digital elevation model for Ts and u to account for the lapse rate; (3) Estimated H is greatly affected by the errors in surface-air temperature differences or surface temperatures measurements; and (4) Ignoring the effect of radiometer viewing angle, can cause variation in Ts by several degrees for some images.

In the computation of sensible heat flex using SEBAL model, the two anchor pixels are take in to account. These are only one that differ SEBAL model from SEBS model.   H and dt are both unknown but are directly related to one another as well as to the value of rah. Therefore, dt is calculated at two extremes, the wettest and driest pixels, by assuming values for H at these reference pixels. The wettest pixel is the pixel where H~0, i.e. all the available energy (Rn-G) is converted λET or dt becomes zero. The driest pixel is the where λET~0, so that H= Rn-G or dt is maximum. The wettest pixels (coldest pixels) are selected in a well-watered agricultural field i.e., at pixels with high NDVI but with low temperature, while the driest pixels (pixels with highest estimated temperature) are selected at pixels with high temperature but with low NDVI and albedo. Water bodies should be avoided during the selection of either pixels due to the problem of lag in stored heat (G) into the body that may not be available at the same instant as Rn or H. Once the wettest and the driest pixels have been selected, temperatures are noted from surface temperature image as Tcold and Thot and locations of the pixels are also noted. Values of Rnhot, Ghot, and rah hot are recorded at the place and Thot is located from the net radiation map, soil heat flux map and aerodynamic resistance map respectively. As the latent heat flux is assumed to be equal to zero at the hottest pixel, the sensible heat flux therefore is equal to the net available energy.

The need to monitor ET at a regional scale is becoming realized as an important matter in studies of global change. As Ayoub (2008) mentioned remote sensing is the only method for effectively and economically estimating ET from a wide area with spatial variation. Methods using Satellite remote sensing data (VIS, NIR, and TIR bands) to derive local, regional and global estimation of turbulent fluxes are a recent development. Among others Surface Energy Balance Algorithm for Land (SEBAL), Two-Source Energy Balance algorithm (TSEB), Surface Energy Balance Index (S-SEBI), Soil Energy Balance System (SEBS) are the most common ones. Among the current satellite remote sensing models, the SEBAL has been designed to calculate the energy portioning at the regional scale with minimum ground data.

SEBAL uses digital imagery data collected by a remote-sensing satellite measuring visible, near infrared and thermal infrared radiation. In the SEBLA model, ET is computed from satellite images and weather data using the surface energy balance. Since the satellite image provides information for the overpass time only, SEBLA computes an instantaneous ET flux for the image time. The ET flux is calculated for each pixel of the image as a “residual” of the surface energy budget equation. The principles and steps needed to apply SEBS to estimate evapotranspiration are described in Bastiaanssen (1995), Bastiaanssen (2003).
Evapotranspiration (ET) is computed as a residual of the energy balance equation on a pixel-by pixel basis:

$$LEpixel = \lambda * ETpixel = Rnpixel - Hpixel - Gpixel \text{……………………………………equation 3.}$$

Where LEpixel: latent heat flux for the pixel, ETpixel: pixel ET, λ: latent heat of vaporization, Rnpixel: the net radiation, Hpixel: sensible heat flux and Gpixel are soil heat flux for each pixel.

The net radiation flux at the surface (Rn) represents the actual radiant energy available at the surface. It is computed by subtracting all outgoing radiant fluxes from all incoming radiant fluxes. This is given in the surface radiation balance equation as follow:

$$Rn = R_S\downarrow - R_S\downarrow + R_L\downarrow - R_L\uparrow - (1 - \varepsilon_{o)}\ R_L\downarrow \ldots\ldots\ldots\ldots\ldots\ldots\ldots\ldots\ldots\ldots\text{equation 4.}$$

RS↓ is incoming shortwave radiation (W/m2), α is broadband surface albedo (dimensionless). RL↓ is incoming long wave radiation (W/m2), RL↑ is outgoing long wave radiation (W/m2), εo is surface thermal emissivity (dimensionless), Rn represents the actual radiant energy available at the surface.

In Equation (4), the amount of shortwave radiation (RS↓) that remains available at the surface is a function of the surface albedo (α). Surface albedo is a reflection coefficient defined as the ratio of the reflected radiant flux to the incident radiant flux over the solar spectrum. It is calculated using satellite image information on spectral radiance for each satellite band. The incoming shortwave radiation (RS↓) is computed using the solar constant, the solar incidence angle, a relative earth-sun distance, and a computed atmospheric transmissivity. The incoming long wave radiation (RL↓) is computed using a modified Stefan-Boltzmann equation with atmospheric transmissivity and a selected surface reference temperature. Outgoing long wave radiation (RL↑) is computed using the Stefan-Boltzmann equation with a calculated surface emissivity and surface temperature. Surface temperatures are computed from satellite image information on thermal radiance.

The surface emissivity is the ratio of the actual radiation emitted by a surface to that emitted by a black body at the same surface temperature. In SEBAL, emissivity is computed as a function of a vegetation index. The final term in Equation (4), (1-εo) RL↓, represents the fraction of incoming long wave radiation that is lost from the surface due to reflection.

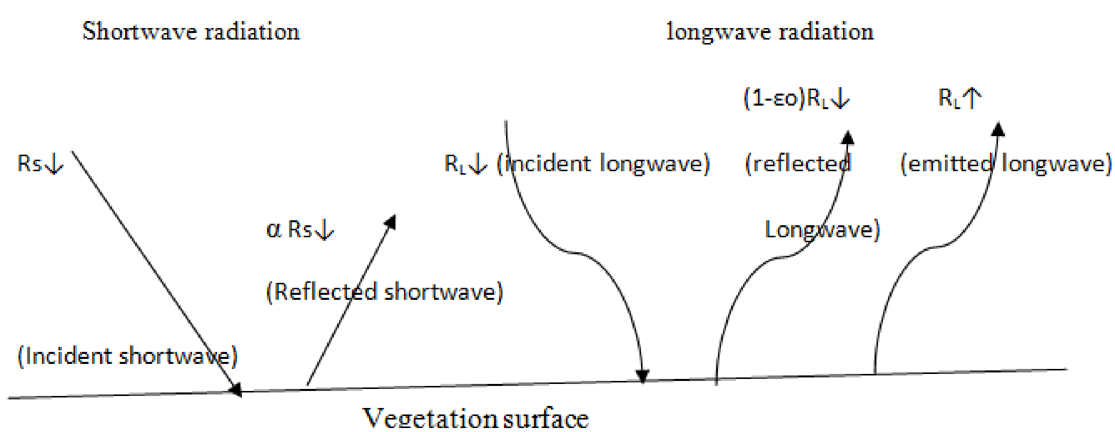

Figure 2.1: Surface radiation balances

Soil heat flux cannot be directly determined from satellite sensors and requires empirical formulation. Remote sensing derivable parameters that influence soil heat flux are used; these include NDVI, surface temperature and albedo

CHAPTER THREE

3. MATERIALS AND METHOD

3.1. Description of the Study Area

3.1.1. Location

The Koga irrigation scheme is a new dam built to irrigate 7000 ha and provide water for irrigation purpose to increase productivity. The storage capacity of the reservoir is 83.1 mm^3.

It is located approximately 35 km southwest of Bahir Dar, the capital of Amhara Region State at an altitude of 1998 m above a msl and approximately 525 km from Addis Ababa, Ethiopia, capital. The catchment is located between $11^o10'$ and $11^o32'$N and $37^o04'$ to $37^o17'$E. The catchment area to the dam is 170.9 km^2 and has an elevation of 901m above a msl (McCartney & Abdo, 2010).

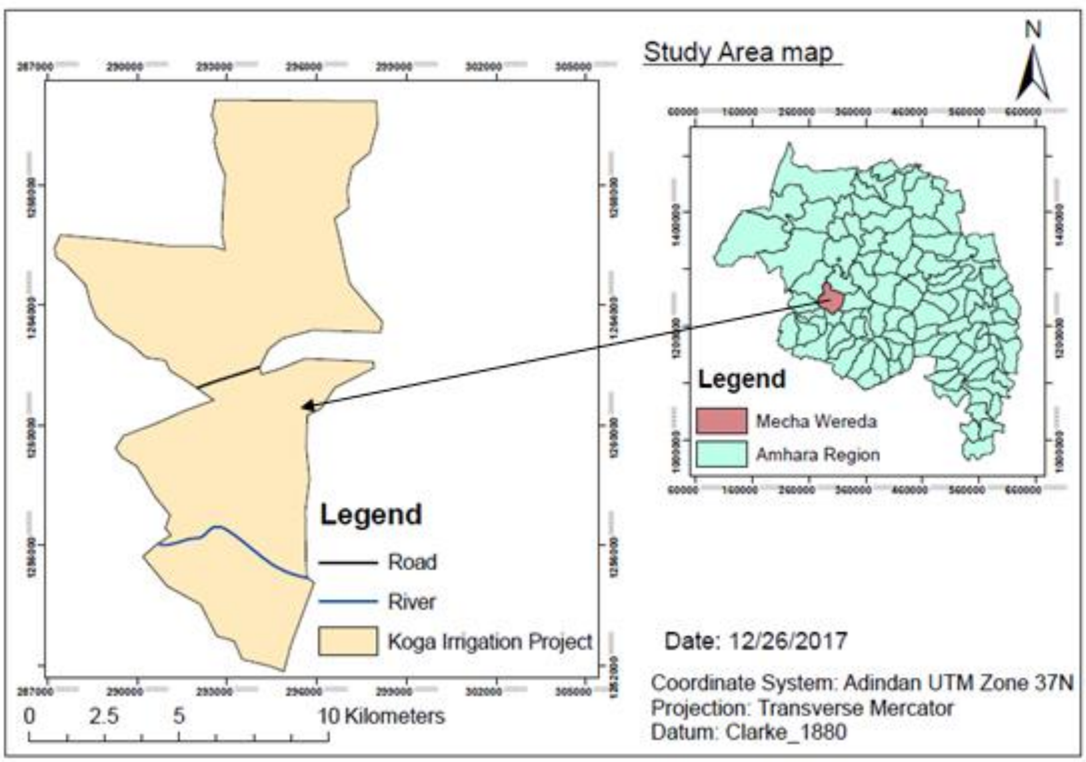

Figure 3.1: Location map of Koga Irrigation Project

3.1.2. Climate Characteristics

3.1.2.1. Rainfall and Temperature

In the study area the minimum, maximum and mean rainfall was 0, 12.95 and 4.08 respectively. The rains usually begin in May and increase gradually in intensity to reach a maximum in July or August. Rainfall declines rapidly after peaking; the cessation of the rains is much more abrupt compared to its onset (MoWR, 2002). The average daytime temperature of the study area was 18.87 ºC. Mean maximum temperature varies from 30.93 ºC in March to 23.4 ºC and 20.34 in August and November respectively; mean minimum temperature varies from 6.15 ºC in November to 14.37 ºC in September. The highest mean temperatures are always between March and May.

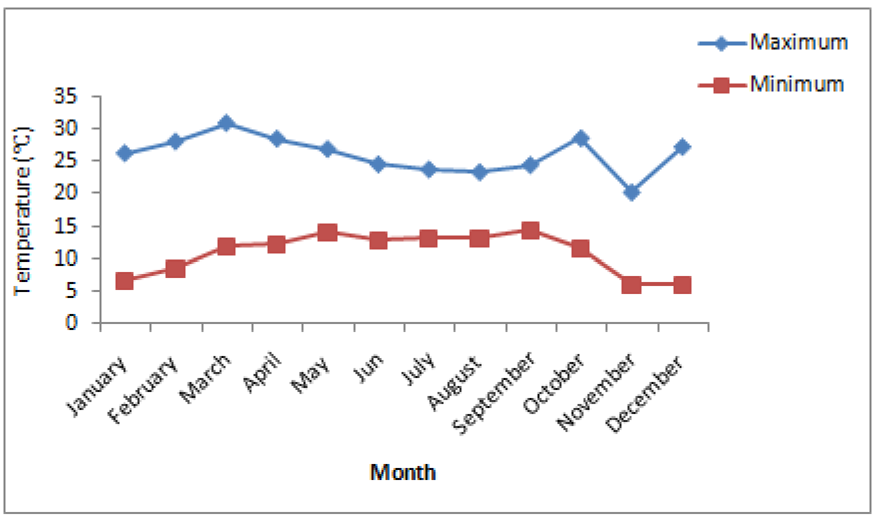

Figure 3.2: The average monthly distribution of temperature of Koga Irrigation Project (2016).

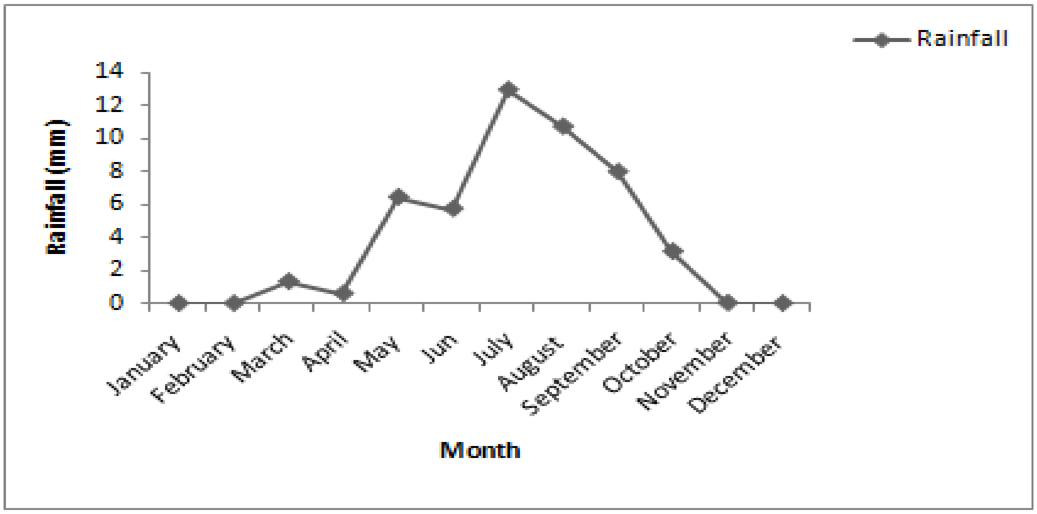

Figure 3.3: The average monthly distribution of rainfall of Koga Irrigation Project (2016).

3.1.2.2. Relative Humidity

Relative humidity is classified as low if it is less than 50%, moderate falls between 50-80% and high is greater than 80%. Accordingly, during most of the months in a year the area is moderate humid. During February, March, April and November are low relative humidity and only in July high relative humidity occurs. The mean monthly relative humidity (RH) is 58.24%; RH values are highest during the humid rainy season (75%) from July to August and lowest during March (42.9%). The variability of RH was also lowest during the wet season. Mean monthly relative humidity of the station is described in figure 3.4 below.

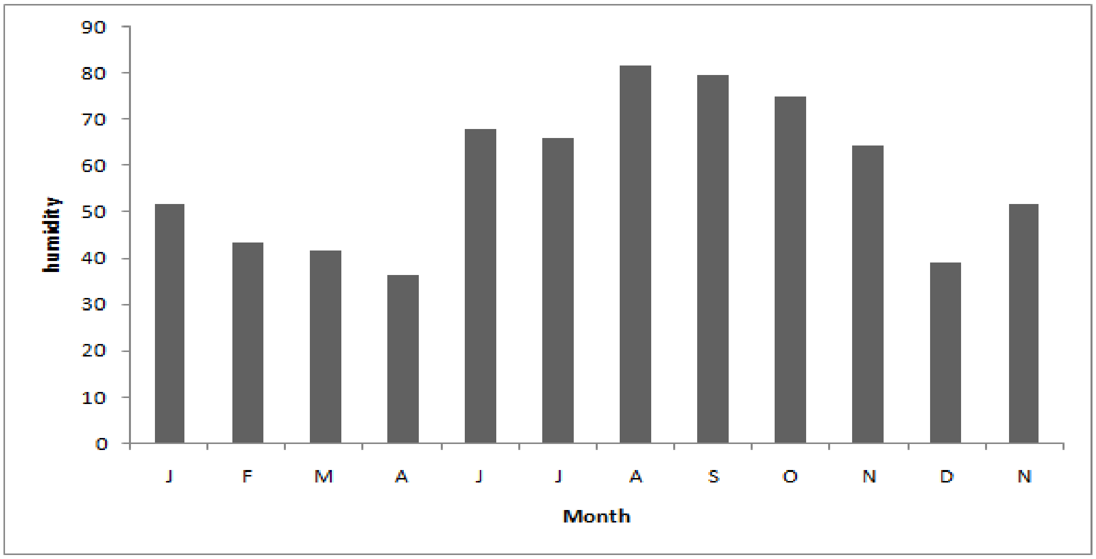

Figure 3.4: Mean monthly distribution of humidity (%) of Koga

3.1.2.3. Wind Speed

The general principal wind direction during dry season, i.e., in the period of February to May is from west to northwest, and wind direction changes at the onset of rainfall. The easterly and southeasterly winds predominate the area beginning from March to May. Months from June to September are dominated by northeaster winds (McCartney & Abdo, 2010). At Koga the highest wind speed (12.15 m/s) occurs in the months of October. Wind speed decreases in August and attain minimum speed in December, January, February and April as shown in figure 3.5 below.

Wind speed, as one of climatologically factors affecting the rate of evapotranspiration and hence the water resource is largely dependent on the source, latitudinal setting, physiographic and vegetation cover of the area(Molla, 2009).

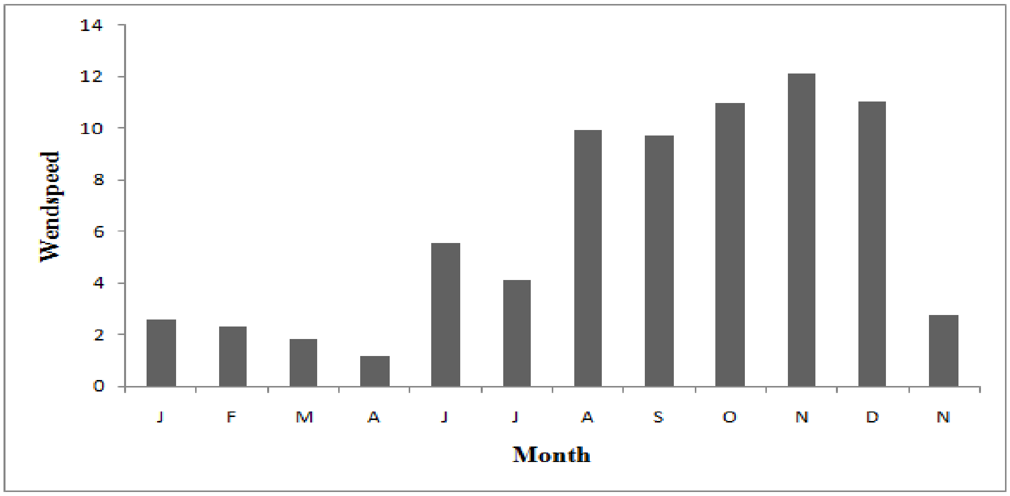

Figure 3.5: Mean monthly distribution of wind speed of Koga (m/s at a height of 2m)

3.1.2.4. Sunshine Hours

The number of daily sunshine hours is one of the climatic factors determining rate of evaporation of water from soil and water bodies. Mean monthly sunshine hour varies from a low value of 4.4 hours per day during the month of August (rainy season) to as high as 9.9 hours per day during the month of December. The average monthly sunshine hour during the year is 7.2 hours per day and its highest variability occurred during the wet season probably because of the frequent sky overcast.

Data on the percentage of twelve hours maximum possible sunshine hours for Koga, average of Bahir Dar and Dangla station, was describe in figure 3.6 below.

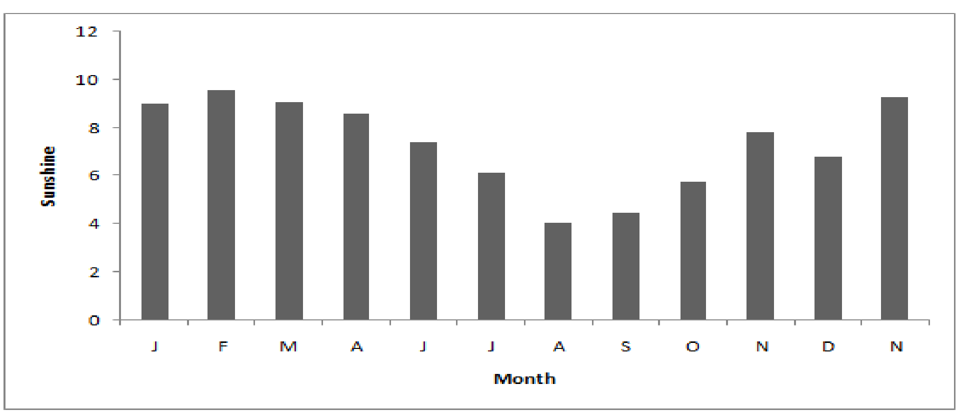

Figure 3.6: Mean monthly distribution of sunshine of Koga (hour)

3.1.3. Geology and Soil of the Study Area

Precambrian rocks formed 600 million years ago form the fundament on which all younger formations are deposited on in Ethiopia. Sedimentary rocks like sandstone, silt and shale were deposited during the Carboniferous–Lower Mesozoic Interval. Previous mismanagement of agricultural land, created soil erosion which has resulted in extensive areas of exposed bedrock (UNESCO, 2004).

The reddish brown soils in the irrigation area are relatively homogeneous and show the same physical and chemical characteristics. As much as 87% of the area is believed to consist of silt clay soils suitable for irrigation. Some expansive paleosols and clays were removed from the canal areas before construction, due to their expansive characteristics, but can still be found in the farmland (MoWR, 2002). Overall the soils are well suited for irrigation, with some exceptions. The lack of nutrients (mainly phosphorous), local abundance of sodium, low pH and a base saturation below 50% are some of the drawbacks.

Haplic Luvisol is the most dominant soil types occupying 91.5% of the study area. These are generally reddish to yellowish brown in color, well drained soils formed in the upland positions mainly in the downstream of the dam site and on both sides of the Koga River. The slopes range from 0 to 8% but are dominantly at 0 to 2%. These soils are intensively cultivated in the study area and possess good drainage and workability. Vertisols are formed in the basins and lower landscape positions on concave slope occupying 4.5% of the study area. They have clay texture throughout the profile and in most cases the proportion of clay fraction is higher (47.5%). The soil cracks widely during the dry season, but the cracks close up again upon re-wetting. The resulting expansion and contraction is responsible for the formation of grooved shiny faces (slickenside) and wedge shape structures at depth (25 to 100 cm). Some of their inherent characteristics cause critical limitations in the study area. Their main constraint is the narrow range of moisture conditions within which mechanical operation can be carried out. Vertisols in the study area are extremely hard when dry, but extremely plastic when wet, this may be associated with the type of clay present which is virtually expanding type. They have problems associated with low permeability and subsurface drainage also. The Gleysols are widespread adjacent to the Vertisols, occupying nearly 286.26 ha (2.8%) of the study area. They are generally lacking the “gilgai” and other vertic characteristics and formed in depressions where ground water is shallow enough to cause permanent water logging. The majority of Gleysols in the study area are under hydrophytes. Cambisols cover only 90.84 ha (1.5%) of the study area (Fig. 2and are developed from recent alluvial deposits along the Koga River in the form of river terraces. The Cambisols within the study area are generally fertile due to occasional flooding and addition of fresh material.

3.1.4. Land Use

Land use of the area is dominated by irrigation crops, rained crops, subsistence peasant farming on individual holdings and traditional grazing on communal lands. The overall farming system is strongly oriented towards cereal production and is dependent on use of oxen for land preparation. The population generally keeps a number of livestock for production of milk by-products and as transferable assets. Crop residue and extensive grazing in the low lying areas are the major contributors to livestock feed resource. In Koga Irrigation Project, approximately 60% of the land area is under intensive cultivation. This number increases to over 80% in the lower watershed, below the proposed dam site. Agriculture in the Koga watershed is dominated by rain fed production of cereals such as tef in lower elevations and barley in higher elevations, pulses such as chickpea and oilseed such as Niger seed as well as finger millet. Grazing is predominantly concentrated in the low lying areas (depression and flood plains). The most commonly harvested crops in dry season at Koga are Maize, Potato and Onion (Mekonen and Kebede, 2011). Based on field observations and discussions made with the local community and district experts, the natural vegetation in the lower watershed and command area is almost completely destroyed due to increased demand in the last decades for fuel wood, construction, timber and agricultural land. The natural vegetations are exist in churches, homestead and in some parts of grazing areas. This destroyed and replaced by man-made vegetations and agricultural crops and some of grazing fields are cover by grasses.

3.2. Data Source

3.2.1. Satellite Image

A LANDSAT 8 OLI_TIRS image (Path 170, Row 052), covering the entire Koga irrigation project, was downloaded from United States Geological Surveying (USGS) website. For these study five months images (January, February, March, April and May of 2016) were downloaded (http: //earthexplorer.usgs.gov).

The remote sensing inputs used for this study are LANDSAT8 OLI_TIRS data having spatial resolution of 30 m for visible and near infrared bands (b1 to b7 and b9) and 100 m resolution for thermal band (b10 and b11) at satellite nadir. The header file for the satellite image is a relatively small file that contains important information for the SEBAL process. Complete summary of imagery is presented on Table 3.1 and 3.2.

Table 3.1: Spectral range and resolution of LANDSAT 8 data

Band	Name	Spectral range	Resolution
1	Coastal/ aerosol	0.435-0.451	30 m
2	Blue	0.452-0.512	30 m
3	Green	0.533-0.590	30 m
4	Red	0.636-0.673	30 m
5	NIR	0.851-0.879	30 m
6	SWIR-1	1.566-1.651	30 m
7	SWIR-2	2.107-2.294	30 m
8	Panchromatic	0.503-0.676	15 m
9	Cirrus	1.363-1.384	30 m
10	TIR-1 (thermal)	10.60-11.19	100 m
11	TIR-2 (Thermal)	11.50-12.51	100 m

Table 3.2: Header files of satellite image for each month

Acquisition Date	Coordinate system	Sun elevation angle (β)	Satellite over pass time and date	Latitude and longitude of the center of the image	
				Latitude	Longitude
2016/01/22	UTM, WGS84 37N	47.08	10:51:45, 2016-01-06	11°34'04.30"N	36°47'57.52"E
2016/02/07	UTM, WGS84 37N	50.768	10:51:43 2016-02-07	11°34'03.61"N	36°47'20.51"E
2016/03/26	UTM, WGS84 37N	62.006	10:51:24, 2016-03-26	11°34'03.65"N	36°47'23.35"E
2016/04/27	UTM, WGS84 37N	65.74	10:51:14, 2016-04-27	11°34'03.11"N	36°45'49.86"E
2016/05/29	UTM, WGS84 37N	64.33	10:51:20, 2016-05-29	11°34'04.33"N	36°47'08.41"E

The satellite overpass time is expressed as Greenwich Mean Time (GMT) and is converted to local time. For LANDSAT 8, the header file includes the LMAX and LMIN for bands 1-7 and 9. These parameters are used to convert digital numbers (DN's) in the original files into energy units. For band 10 and 11, the thermal band, both LMAX and LMIN images are supplied is recommended to use for SEBA to compute surface temperature.

3.2.2. Weather Data

The methods for calculating evapotranspiration from meteorological data require various climate parameters. The meteorological factors determining evapotranspiration are weather parameters which provide energy for vaporization and remove water vapor from the evaporating surface. The principal weather parameters that can be considered to estimating evapotranspiration in this study are temperature, precipitation, wind speed, humidity and sunshine. This meteorological data, from Dangla and Bahir Dar metrological stations, were obtained from the National Meteorological Agency for the year 2016. Hourly and daily data, at the time of satellite overpass, were used in SEBAL processing are described in the following table.

Table 3.3: Average daily weather conditions at the time of satellite overpass

Satellite overpass time at local time	Weather at time of satellite overpass				
	Temperature (^{o}c)	Humidity (%)	Daily precipitation (mm)	Wind speed at 2m(m/s)	Daily Sunshine (hours)
2016/01/22, 10:51:45	17.4	55	0	1.2	8.7
2016/02/07, 10:51:43	18	51.5	0	1.82	10.1
2016/03/23, 10:51:24	21.87	32	0	0.95	9.35
2016/04/27, 10:51:14	22.55	45	1.8	1.98	8.3
2016/05/29, 10:51:20	21.025	68.5	5.95	2.73	8

3.2.3. Materials

Different materials and software are used to undertake this research. The following table described software's and its application which is used to perform different activities.

Table 3.4: software and its application in the study

Software	Application
ERDAS imagine 10.3	➢ To estimate NDVI, SAVI, LAI, Ts, surface albedo, surface emissivity, net surface radiation flux, soil heat flux, sensible heat flux and evapotranspiration using ERDAS model maker. ➢ Used to layer stake, Land use classification
Excel with XLSTAT 2017	➢ Used to generate charts, tables and some correlation of different parameters and out puts.
CROPWAT 8.0	➢ To estimate evapotranspiration from weather data using FAO method, to calculate crop water requirement and to compute irrigation water requirement and irrigation schedules of different crops and vegetables in the study area.
ARC GIS	➢ Calculate LST, NDVI, SAVI, cartographic map purpose ➢ Develop study area map,

3.3. Methods

3.3.1. SEBAL Model

The SEBAL model was used to estimate ET using ERDAS imagine model maker. To calculate ET net surface radiation, soil heat flux, latent heat flux, latent heat of vaporization and sensible heat flux was used as input. Evapotranspiration (ET) is computed as a residual of the energy balance equation on a pixel-by pixel basis using more than 35 equations.

To calculate the ET using SEBAL method, the required mathematical equations for building the algorithms of processing and analysis models are collected. Sixteen spatial analysis models are prepared using ERDAS imagine software i.e. atmospheric correction models for calculating the reflectance, surface albedo, emissivity, surface temperature, and elements of solar radiations balance, including net radiations, soil heat flux, sensible heat flux, latent heat flux, and finally calculating the instantaneous and daily actual evapotranspiration values.

The formula have been used to estimate ET using ERDAS model maker based on SEBAL model are in equation (1) as : $LEpixel = \lambda * ETpixel = Rnpixel - Hpixel - Gpixel$

Where LEpixel: latent heat flux for the pixel, ETpixel: pixel ET, λ: latent heat of vaporization, Rnpixel: the net radiation, Hpixel: sensible heat flux and Gpixel are soil heat flux for each pixel.

3.3.2. Penman-Monteith (FAO) Method

Reference evapotranspiration was estimated using FAO method from weather data that are taken from Dahir Dar and Dangela stations. In this study, crop evapotranspiration and crop water requirement was estimated using Cropwat8 software and it is used temperature, rain fall, humidly, sunshine, wind speed and soils as input parameter in the computation process. The following diagrams show the overall procedures in the computation of evapotranspiration and irrigation performance indicators and finally assess the performance of irrigation project.

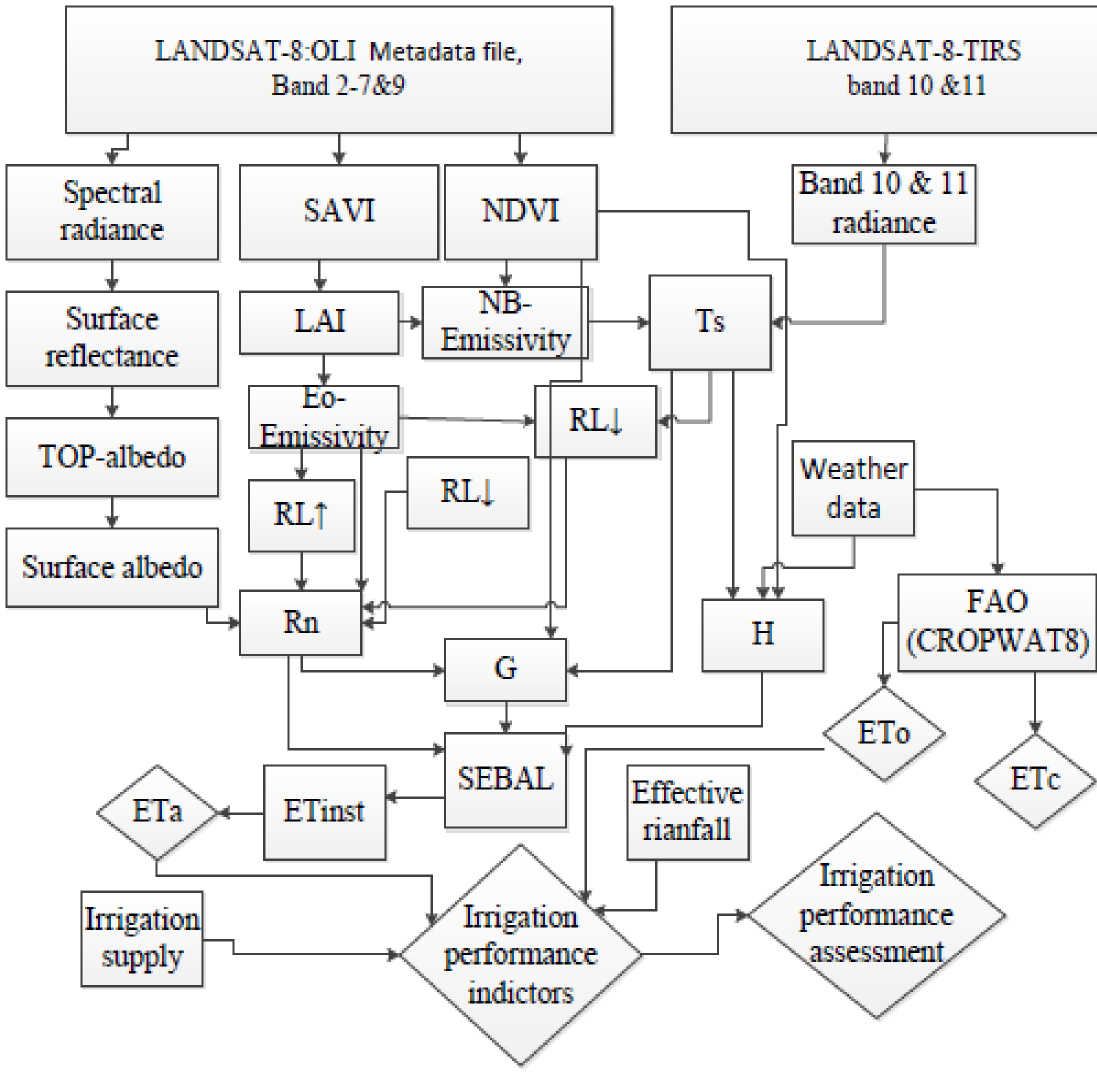

Figure 3.7: Overall schema of the study

3.3.3. Remote Sensing Based Data Analysis

3.3.4. Satellite Image for SEBAL Model

The satellite image for the area of interest was downloaded from United Sates Geological Surveying (USGS) sites. The satellite image is already Geo-referenced and terrain corrected in UTM, WGS84 37N. The layered spectral band image is created from the geo-rectified disk using ERDAS Imagine software, in order from band1 to band 7, necessary for the SEBAL procedure. Once a layered image is produced, a subset image is created if a smaller area is to be studied. The header file information like Overpass date and time, Latitude and Longitude of image center, Sun elevation angle at overpass time, earth-sun distance, LMAX and LMIN of each band (LANDSAT 8) was obtained from the LANDSAT metadata files which are used as input for farther computation. Weather data like temperature, rainfall, wind speed, humidity and sunshine from Bahir Dar and Dangla weather station and organized it in a table format.

3.3.5. SEBAL Model Procedures for Evapotranspiration Computation

Surface Energy Balance Algorithm for Land, developed by Bastiaanssen (2000), was formulated to estimate evapotranspiration at the time of satellite overpass from remotes sensing images. The estimation of evapotranspiration form remote sensing data using SEBAL model has a series of steps. The computation of evapotranspiration based on the model was used net surface radiation (Rn), soil heat fluxes (G) and sensible heat flux (H) as input parameters and the computation of each parameter has also its own procedures. These parameters were computed using both ERDAS imagine model maker and ARC GSI raster calculator by follow a series of steps. So, in the data processing and analysis part the computing procedure of each parameter are described with its output (results) as follow.

3.3.5.1. Net Surface Radiation Flux (Rn)

Net radiation budget is the total amount of radiation left after all the outgoing radiation fluxes are subtracted from the incoming radiation fluxes. Net surface radiation was estimated by following procedures presented by Bastiaanssen *et al* (2000) as:

$$R_n = (1-\alpha)\, R_{S\downarrow} + R_{L\downarrow} - R_{L\uparrow} - (1-\varepsilon_o)\, R_{L\downarrow} \quad \ldots\ldots 5$$

Where Rn = net surface radiation flux, α = surface albedo, $R_S\downarrow$ = short wave incoming radiation, $R_L\downarrow$ = long wave incoming radiation, $R_L\uparrow$ = long wave outgoing radiation and ε_o = surface emissivity. It was further estimated by a series of modeling techniques presented in the following diagram.

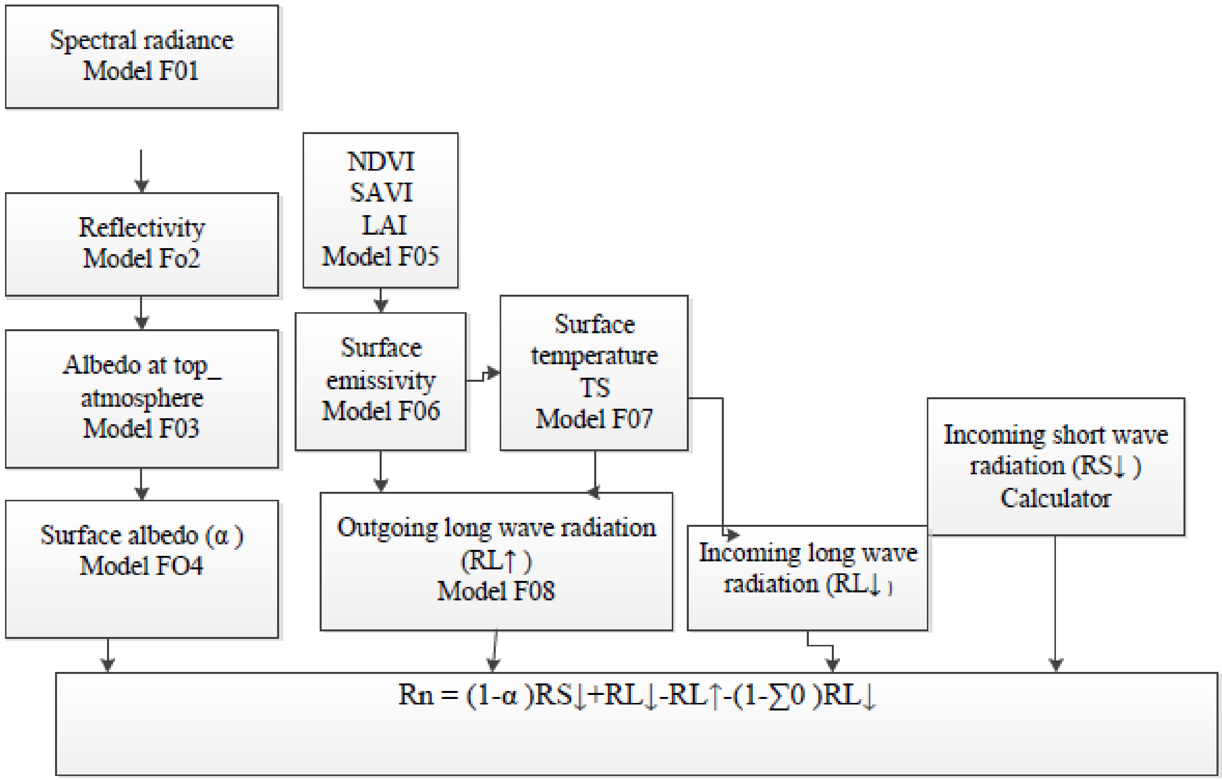

Figure 3.8: Flow Chart of the Net Surface Radiation Computation

The incoming shortwave radiation ($R_{S\downarrow}$) was computed with a spreadsheet or a calculator rather than the Model Maker tool. Surface albedo, shortwave incoming radiation, long wave incoming radiation, long wave outgoing radiation and surface emissivity was used as input parameter to compute net surface radiation. The parameters used as input to compute net surface radiation flux are computed step by step using ERDAS model maker and raster calculator in ARC GIS as follow.

3.3.5.2. Surface Albedo

Surface albedo is the fraction of the incident sunlight that the surface reflects. It is easily computed in SEBAL through the following steps:

A. The spectral radiance for each band (L_λ) is computed (model F01) as shown in Figure 8. This is the outgoing radiation energy of the band observed at the top of the atmosphere by the satellite. It is calculated using the following equations presented by Bastisansen *et al* (2000) as,

$$L\lambda = \left[\frac{(LMAX - LMIN)}{(QCALMAX - QCALMIN)}\right](DN - QCALIM) + LMIN \ldots\ldots\ldots\ldots\ldots\ldots\ldots\ldots\ldots\ldots 6$$

Where; DN is the digital number of each pixel, LMAX and LMIN are calibration constants, QCALMAX and QCALMIN are the highest and lowest range of values for rescaled radiance in DN and we can get its value from the metadata of the image. The value of QCALMAX and QCALMIN for LANDSAT8 was 65,535 and 1 respectively. The units for L_λ are W/m^2/sr/µm.

B. The reflectivity for each band (ρ_λ) is computed based on model F02 from figure 8. The reflectivity of a surface is the ratio of the reflected radiation flux to the incident radiation flux. It is computed based on the equation presented by Bastisansen *et al* (2000) as:

$$P\lambda = \frac{((\pi.L\lambda))}{(ESUN\lambda.\cos\theta.dr)} \ldots\ldots\ldots\ldots\ldots\ldots\ldots\ldots\ldots\ldots\ldots\ldots\ldots\ldots\ldots\ldots 7$$

where; L_λ is the spectral radiance for each band computed in equation 6, $ESUN_\lambda$ is the mean solar exo-atmospheric irradiance for each band (W/m^2/µm), cos θ is the cosine of the solar incidence angle (from nadir), and d_r is the inverse squared relative earth-sun distance. Exo-atmospheric irradiance value of each band of LANDSAT8 images have been taken from http://landsat.usgs.gov/band_designations_landsat_satellite.php sites (Table 3.5). Cosine θ is computed using the header file data on sun elevation angle (β) where θ = (90^0 - β). The term d_r is computed as $1/d_{e-s}^2$ where d_{e-s} is the relative distance between the earth and the sun in astronomical units and gets its value from the metadata of the image.

C. The albedo at the top of the atmosphere (α_{toa}) is computed in model F03 as show in figure 8. It is the albedo unadjusted for atmospheric transmissivity and is computed by the equation presented by Bastisansen *et al* (2000) as follows:

$$\alpha_{toa} = \sum(\omega_\lambda \times \rho_\lambda) \ldots\ldots\ldots\ldots\ldots\ldots\ldots\ldots\ldots\ldots\ldots\ldots\ldots\ldots 8$$

Where; ρ_λ is the reflectivity computed in equation 7 and ω_λ is a weighting coefficient for each band computed as follows (Bastisansen *et al*, 2000):

$$\omega\lambda = \frac{\mathrm{ESUN}\lambda}{\sum \mathrm{ESUN}\lambda} \quad \ldots 9$$

Table 3.5: ESUN and weighting coefficient of bands of LANDSAT8

Band	2	3	4	5	6	7
ESUN	2067	1893	1603	972.6	245	79.72
wλ	0.301297899	0.27593465	0.23366257	0.141771812	0.03571262	0.011620449

Source: http://landsat.usgs.gov/band designations Landsat satellite.php

D. The final step is to compute the surface albedo in model F04 in figure 8. Surface albedo is computed by correcting the albedo at the top of the atmosphere for atmospheric transmissivit. It is computed based on the equation presented by Bastisansen *et al*, 2000 as:

$$\alpha = \frac{\left(\alpha_{toa} - \alpha_{path_{radiance}}\right)}{\tau_{sw}{}^{2}} \quad \ldots 10$$

Where; $\alpha_{path\_radiance}$ is the average portion of the incoming solar radiation across all bands that are back-scattered to the satellite before it reaches the earth's surface, and τ_{sw} is the atmospheric transmissivity.

Values for $\alpha_{path\_radiance}$ range between 0.025 and 0.04 and for SEBAL study considered a value of 0.03 based on Bastiaanssen *et al (*2000). Atmospheric transmissivity is defined as the fraction of incident radiation that is transmitted by the atmosphere and it represents the effects of absorption and reflection occurring within the atmosphere. This effect occurs to incoming radiation and to outgoing radiation. τ_{sw} includes transmissivity of both direct solar beam radiation and diffuse (scattered) radiation to the surface. τ_{sw} were calculate assuming clear sky and relatively dry conditions using an elevation-based relationship (Allen *et al*., 1998):

$$\tau_{sw} = 0.75 + 2 \times 10^{-5} \times Z \qquad \ldots 11$$

Where; z is the elevation above sea level (m). This elevation should best represent the area of interest, such as the elevation of the relevant weather station that is used in this study and in this study the value of Z is 1998 m which is the elevation of Bahir Dar station.

3.3.5.3. Incoming Shortwave Radiation ($R_{S\downarrow}$)

Incoming shortwave radiation is the direct and diffuse solar radiation flux that actually reaches the earth's surface (W/m^2). It is calculated, by assuming clear sky conditions, as a constant for the image time and computed using the following equation (Bastisansen *et al*, 2000):

$$R_S \downarrow = G_{sc} \times \cos\theta \times dr \times \tau_{sw} \qquad \ldots 12$$

Where; G_{sc} is the solar constant (1367 W/m^2), cos θ is the cosine of the solar incidence angle as θ is computed by subtracting sun elevation angle from 90^o , d_r is the inverse squared relative earth-sun distance, and τ_{sw} is the atmospheric transmissivity and computed based on equation 11. These calculations are done with a spreadsheet or simply use a calculator. Values for $R_{s\downarrow}$ can range from 200 – 1000 W/m^2 depending on the time and location of the image. In this study the computed value of incoming shortwave radiation based on equation 12 are 831.56, 860.009, 896.33, 971.59 and 947.29 for January 22, February 7, March 23, April 27 and May 29 respectively.

3.3.5.4. Outgoing Long Wave Radiation ($R_{L\uparrow}$)

The outgoing long wave radiation is basically the thermal radiation flux computed from the earth's surface to the atmosphere (W/m^2). It is computed in SEBAL through the following steps using equation 18 (Bastisansen *et al*, 2000). These steps are described as follows.

1. Vegetation Indices

Three commonly used vegetation indices are computed in model F05 as show in figure 8. These indices are Normalized Difference Vegetation Index (NDVI), Soil Adjusted Vegetation Index (SAVI), and Leaf Area Index (LAI). Any one of these indices can be used to predict various characteristics of vegetation, according to preferences of the user.

1. Normalized Difference Vegetation Indices (NDVI)

The NDVI is the ratio of the differences in reflectivity for the near-infrared band (B_5) and the red band (B_4) for LANDSAT 8 and computed using the following equation (Schell, J, 1973):

$$\mathrm{NDVI} = \frac{(B_5 - B_4)}{(B_5 + B_4)} \qquad \ldots 13$$

Where; B_5 and B_4 are reflectivity for bands 5 and 4 respectively. The NDVI is a sensitive indicator of the amount and condition of green vegetation. Values for NDVI range between -1 and +1. Green surfaces have a NDVI between 0 and 1 and water and cloud are usually less than zero that is between 0 and -1.

2. Soil Adjusted Vegetation Indices (SAVI)

The SAVI is an index that attempts to "subtract" the effects of background soil from NDVI. So, that impact of soil moisture is reduced in the index. It is computed as the equation formulated by Hute, A.R. (1988).

$$\mathrm{SAVI} = \frac{[(1+L)(B_5 - B_4)]}{(L + B_5 + B_4)} \qquad \ldots 14$$

Where; L is a constant for SAVI. If L is zero, SAVI becomes equal to NDVI. A value of L is 0.5 frequently appears (Bastisansen *et al*, 2000).

3. Leaf Area Indices (LAI)

The LAI is the ratio of the total area of all leaves on a plant to the ground area represented by the plant. It is an indicator of biomass and canopy resistance. LAI is computed based on the following empirical equation (Bastisansen *et al*, 2000): it is done using raster calculator in ARC GIS.

$$\mathrm{LAI} = -\left(\frac{\ln\left(\frac{0.69-\mathrm{SAVI}}{0.59}\right)}{0.91}\right)\ldots\ldots\ldots 15$$

3.3.5.5. Surface Emissivity

Surface emissivity (ε) is the ratio of the thermal energy radiated by the surface to the thermal energy radiated by a blackbody at the same temperature. There are two surface emissivities which are used in SEBAL. The first represented surface behavior for thermal emission in the relatively narrow band 10 and 11 (10.4 to 12.5 μm), expressed as ε_{NB}. The second represented surface behavior for thermal emission in the broad thermal spectrum (6 to 14 μm), expressed as ε_o. ε_{NB} is used in calculation of surface temperature (Ts) and ε_o is used later on to calculate total long wave radiation emission from the surface and also computed net surface radiation.

According to Bastisansen *et al*, (2000) surface emissivity is computed using the following empirical equations depends on the relationship of NDVI, LAI and albedo.

- ε_{NB} = 0.97 + 0.0033 LAI; when LAI < 3 and NDVI > 0 or ε_{NB} = 0.98; when LAI >= 3 and NDVI >0 or ε_{NB} = 0.985; when NDVI < 0 and albedo < 0.47 ………………… (16a)
- ε_0 = 0.95 + 0.01 LAI; when LAI < 3 and NDVI > 0 or ε0 = 0.98; when LAI ≥ 3 and NDVI > 0 or ε_o = 0.985; when NDVI < 0 and albedo < 0.47…………………..…… (16b)

Surface Temperature

The surface temperature (Ts) is computed in model F07 based on the modified Plank equation as follow:

$$\mathrm{TS} = \mathrm{K2}/\ln\left(\left(\varepsilon\mathrm{NB}\frac{\mathrm{K1}}{\mathrm{Rc}}\right) + 1\right)\ldots\ldots\ldots 17$$

Where; Rc is the thermal radiance from the surface from model F01. K_1 and K_2 are constants for LANDSAT 8 images which are found in the metadata of the image. Units for Rc must be the same as those for K1 and its value is equal to the spectral radiance of band10 and band11 (thermal band) and εNB is emissivity of band 10 and band 11 computed from equation 16a.

So, outgoing long wave radiation ($R_{L\uparrow}$) is computed (model F08) based on the equation presented by Stefan-Boltzmann equation as:

$$RL\uparrow = \varepsilon_o \times \sigma \times T_S^4 \ldots\ldots 18$$

Where; ε_o is the "broad-band" surface emissivity computed in equation 16b above (dimensionless), σ is the Stefan-Boltzmann constant (5.67×10^{-8} W/m^2/K^4), and T_s is the surface temperature (K) computed in equation 17.

3.3.5.6. Long Wave Incoming Radiation ($R_{L\downarrow}$)

The long wave incoming radiation is the downward thermal radiation flux from the atmosphere (W/m^2). It is computed using the Stefan-Boltzmann equation as:

$$RL\downarrow = \varepsilon a \times \sigma \times T_S^4 \ldots\ldots 19$$

Where **σ** is the Stefan-Boltzmann constant (5.67×10^{-8} W/m^2/K^4), and T_s is the near surface air temperature (K) computed in equation 17. Atmospheric emissivity was computed the empirical equation presented by Bastiaanssen (1995) as:

$$\varepsilon a = 0.85 \times (-\ln \tau sw)^{0.09} \ldots\ldots 20$$

Where; τ_{sw} is the atmospheric transmissivity calculated from Equation 11. Long wave incoming radiation was done simply using a raster calculator on ARC GIS as follow,

0.7464 * (5.67/100000000) * ("ts.img" * "ts.img" * "ts.img" * "ts.img") done in raster calculator in ARC GIS. Where, TS stands surface temperature.

4.3.4. Soil Heat Flux

The soil heat flux (G) and sensible heat flux (H) of the surface energy budget equation was computed after net surface radiation flux is estimated. The net radiation flux (R_n) is the net amount of radiant energy that is available at the surface for warming the soil, warming the air, or evaporating soil moisture. According to Bastisansen *et al,* (2000) the surface energy budget equation is:

$$\mathrm{Rn} = \mathrm{G} + \mathrm{H} + \lambda\mathrm{ET}\ldots\ldots\ldots\ldots\ldots\ldots\ldots\ldots\ldots\ldots\ldots\ldots\ldots\ldots\ldots\ldots\ldots\ldots\ldots\ldots\ldots 21$$

Where; R_n is the net radiation at the surface (W/m^2), G is the soil heat flux (W/m^2), H is the sensible heat flux to the air (W/m^2), and λET is the latent heat flux (W/m^2).

Soil heat flux is the rate of heat storage in the soil as a result of the temperature gradient between the soil heat surface and the underlying soil layers. The temperature gradient varies with the fractional vegetation cover and the leaf area index, as the light intersection from and shadow formation on the bare soil determine relative heating of the bare soil surface. Due to lack of spatial information about thermal conductivity of soil the empirical relationship developed by Bastiaanssen (1995) has been applied, it calculates soil heat flux as a function of Rn, NDVI, broad band albedo and surface temperature:

$$\mathrm{G} = \mathrm{Rn} - \left(\frac{\mathrm{TS}-273}{\alpha}\right)(0.0038\alpha + 0.0074\alpha^2)(1 - 0.98\mathrm{NDVI}^4)\ldots\ldots\ldots\ldots\ldots\ldots\ldots\ldots\ldots\ldots\ldots 22$$

Where; Rn is net radiation (Wm-2), Ts is surface temperature (°K), **α** is broad band surface albedo and NDVI is vegetation index normalized differential vegetation index.

Soil heat flux is a difficult term to evaluate and care should be used in its computation. One must understand the area of interest in order to evaluate the accuracy of Equation (22). Values of G should be checked against actual measurements on the ground. Land classification and soil type will affect the value of G and a land-use map is valuable for identifying the various surface types. Files for NDVI, surface temperature, surface albedo, and R_n are entered and the output files and model are saved.

4.3.5. Sensible Heat Flux (H)

Sensible heat flux is the rate at which energy loss from soil through convection and diffusion process as a result of temperature difference between the surface and the lowermost overlaying atmosphere. It is estimated from surface temperature, surface roughness and measured wind speed by following method presented by Bastisansen *et al*, (2000):

$$H = \frac{\rho \times C_P \times dT}{r_{ah}} \text{...} 23$$

Where; ρ is air density (kg/m^3) computed online using temperature and wind speed, c_p is air specific heat (1004 J/kg/K), dT (K) is the temperature difference ($T_1 - T_2$) between two heights (z_1 and z_2), and r_{ah} is the aerodynamic resistance to heat transport (s/m).

The sensible heat flux (H) is a function of the temperature gradient, surface roughness, and wind speed. Equation (23) is difficult to solve because there are two unknowns, r_{ah} and dT. To facilitate this computation, we need to use the two "anchor" pixels (where reliable values for H can be predicted and a dT estimated) and the wind speed at a given height.

The aerodynamic resistance to heat transport (r_{ah}) is computed using z_1, z_2, k and u_* use as inut based on equation (24). A series of iterations is required to determine the value for r_{ah} for each period that considers the impacts of buoyancy on rah and H. Based on experienced analysis, for agricultural area the values of 0.1 meter and 2.0 meters are assign for z_1 and z_2 respectivelly· (Bastiaanssen,2002). Based on Karman's, equation aerodynamic resistance to heat transport (r_{ah}) is computed as:

$$r_{ah} = \ln\left(\frac{Z_2}{Z1}\right) / (U_* \times K) \text{ ....} 24$$

Where; z_1 and z_2 are heights in meters above the zero plane displacement (d) of the vegetation, u_* is the friction velocity (m/s) which quantifies the turbulent velocity fluctuations in the air, and k is von Karman's constant (0.41). The friction velocity (u_*) is computed using the logarithmic wind law for neutral atmospheric conditions:

$$U_* = (KU_X)/\ln(Z_X/Z_{om}) \text{...} 25$$

Where; k is von Karman's constant, u_x is the wind speed (m/s) at height z_x, and z_{om} is the momentum roughness length (m). The calculation of u_* requires a wind speed measurement (u_x) at a known height (z_x) at the time of the satellite image. This measurement is taken from the weather data that was set up earlier in the SEBAL process. The momentum roughness length (z_{om}) is empirically estimated from the average vegetation height around the weather station using the following equation (Brutsaert, 1982):

$$Z_{om} = 0.12h \ldots\ldots 26$$

For agricultural areas, z_{om} is calculated as a function of Leaf Area Index (LAI):

$$Z_{om} = 0.018LAI \ldots\ldots 27$$

Where; LAI is leaf area index computed in equation (14). This calculation is done simply using raster calculator in ARC GIS.

The temperature difference dt is calculated from following equation:

$$dt = \frac{Hrah}{p_a c_p} \ldots\ldots 28$$

In this equation H and dt are both unknown but are directly related to one another as well as to the value of rah. Therefore, dt is calculated at two extremes, the wettest and driest pixels, by assuming values for H at these reference pixels. The wettest pixel is the pixel where H~0, i.e. all the available energy (Rn-G) is converted λET or dt becomes zero. The driest pixel is the where λET~0, so that H= Rn-G or dt is maximum. The wettest pixels (coldest pixels) are selected in a well-watered agricultural field i.e., at pixels with high NDVI but with low temperature, while the driest pixels (pixels with highest estimated temperature) are selected at pixels with high temperature but with low NDVI and albedo. Water bodies should be avoided during the selection of either pixels due to the problem of lag in stored heat (G) into the body that may not be available at the same instant as Rn or H. Once the wettest and the driest pixels have been selected, temperatures are noted from surface temperature image as Tcold and Thot and locations of the pixels are also noted. Values of Rnhot, Ghot, and rahhot are recorded at the place and Thot is located from the net radiation map, soil heat flux map and aerodynamic resistance map respectively. As the latent heat flux is assumed to be equal to zero at the hottest pixel, the sensible heat flux therefore is equal to the net available energy:

$$H_{hot} = Rn_{hot} - G_{hot} \ldots\ldots 29$$

Temperate difference (dt) is then calculated from the following equation:

$$dt_{hot} = \frac{(h_{hot} \times rah_{hot})}{pa \times 1004} \ldots\ldots 30$$

Where; dthot Values of Tcold, Thot, and dthot are known and may be used to apply the following equation:

$$T_{hot} - T_{cold} = dt = a + bT_S \ldots\ldots\ldots\ldots\ldots\ldots\ldots\ldots\ldots\ldots\ldots\ldots\ldots\ldots\ldots\ldots\ldots\ldots\ldots\ldots \ldots 31$$

After solving for "a" and "b", the sensible heat flux (H) for the whole image is calculated iteratively until convergence in the successive value is found. Finally, the latent heat flux (λET) is computed for each pixel as a residual term of the surface energy balance. An equivalent amount of instantaneous ET is also calculated by dividing the latent heat flux by the latent heat of vaporization (λ).

4.3.6. Latent Heat Flux (**λE**)

Latent heat flux is the rate of latent heat loss from the surface due to evapotranspiration. It can be computed for each pixel using Equation presented by Bastisansen *et al*, (2000) as:

$$\lambda E = R_n - G - H \ldots\ldots\ldots\ldots\ldots\ldots\ldots\ldots\ldots\ldots\ldots\ldots\ldots\ldots\ldots\ldots\ldots\ldots\ldots\ldots\ldots\ldots\ldots\ldots\ldots\ldots\ldots\ldots\ldots\ldots\ldots\ldots\ldots 32$$

Where; λE is latent heat flux, which is the residual radiation, value at the time of the satellite overpass (W/m^2). According to Bastisansen *et al*, (2000) equation the instantaneous value of ET in equivalent evaporation depth is computed as:

$$ET_{inst} = \frac{3600\lambda E}{\lambda} \ldots\ldots\ldots\ldots\ldots\ldots\ldots\ldots\ldots\ldots\ldots\ldots\ldots\ldots\ldots\ldots\ldots\ldots\ldots\ldots\ldots\ldots\ldots\ldots 33$$

Where; ET_{inst} is the instantaneous ET (mm/hr), 3600 is the time conversion from seconds to hours, and λ is the latent heat of vaporization or the heat absorbed when a kilogram of water evaporates (J/kg).

$$\lambda = 2501 - 0.00236(T_S - 273) * 10^6 \ldots\ldots\ldots\ldots\ldots\ldots\ldots\ldots\ldots\ldots\ldots\ldots\ldots\ldots\ldots\ldots\ldots\ldots\ldots\ldots\ldots 34$$

Where: Ts is the surface temperature chart (oC) obtained from the thermal band of landsat8 as estimated in equation 17. With the radiation balance, soil heat flux and latent heat flux charts, the evaporative fraction was obtained and expressed by the equation (Allen, 2002):

$$\Delta = \frac{LET}{Rn - G} \ldots\ldots\ldots\ldots\ldots\ldots\ldots\ldots\ldots\ldots\ldots\ldots\ldots\ldots\ldots\ldots\ldots\ldots\ldots\ldots\ldots\ldots\ldots\ldots\ldots\ldots\ldots\ldots\ldots\ldots\ldots\ldots\ldots 35$$

The evaporative fraction has an important characteristic, it regularity and constancy in clear sky days. In this sense, we can admit that it's instantaneously character represents its diurnal mean value satisfactorily, enabling the estimation of daily evapotranspiration by the equation:

$$\mathrm{ET_{24h}} = \frac{86400\Delta \mathrm{Rn_{24h}}}{\lambda} \ldots \ldots \ldots \ldots \ldots \ldots \ldots \ldots \ldots \ldots \ldots \ldots \ldots \ldots \ldots \ldots \ldots \ldots \ldots \ldots \ldots \ldots \ldots \ldots \ldots \ldots \ldots .36$$

Where: Rn24h, is the mean radiation balance occurred during a period of 24 hours, expressed in W.m-2, obtained by the equation (Allen, 2002):

$$\mathrm{Rn_{24h}} = (1-\alpha)\mathrm{R}s_{\mathrm{24h}} - 110\tau_{\mathrm{sw}_{\mathrm{24h}}} \ldots \ldots \ldots \ldots \ldots \ldots \ldots \ldots \ldots \ldots \ldots \ldots \ldots \ldots \ldots \ldots \ldots \ldots \ldots \ldots \ldots \ldots 37$$

Whereα, which is surface albedo, and $\tau_{\mathrm{sw}_{\mathrm{24h}}}$is estimated in equation 10 and 11 respectively.

Allen *et al*. (2002) defined the evaporative fraction of reference (ETrF) as the relation between the ETinst chart and the ETo (ET_{FAO56}) integrated at the same moment and computed with data obtained from a meteorological station is:

$$\mathrm{ETrF} = \frac{\mathrm{ET_{inst}}}{\mathrm{ET_{FAO56}}} \ldots \ldots \ldots \ldots \ldots \ldots \ldots \ldots \ldots \ldots \ldots \ldots \ldots \ldots \ldots \ldots \ldots \ldots \ldots \ldots \ldots \ldots \ldots \ldots \ldots \ldots \ldots .38$$

And also in addition to equation 24 ET_{24h} is computed by the equation presented by Allen (2002) as:

$$\mathrm{ET_{24h}} = \mathrm{ETrF} * \mathrm{ET_{024}} \ldots \ldots \ldots \ldots \ldots \ldots \ldots \ldots \ldots \ldots \ldots \ldots \ldots \ldots \ldots \ldots \ldots \ldots \ldots \ldots \ldots \ldots \ldots \ldots \ldots \ldots \ldots \ldots 39$$

4.4. Estimation of Water Requirement

4.4.1. Estimation of Crop Water Requirement

Water used by crops is predominantly lost by transpiration (T) but there are also evaporative (E) losses from the soil and from plant surfaces. The amount of water used by plants together with water losses through evaporation is called evapotranspiration (ET). Other potential areas of water loss during irrigation include lateral run off, deep drainage and leaks in the delivery system. These are not directly accounted for in ET calculations, but can be measured and included in estimates of crop irrigation requirements. ETo is used as a reference point from which crop ET (termed ETc) can be calculated by multiplying ETo by crop coefficient value. The water requirements of a crop can be compared with the ETo by using an experimentally-derived crop coefficient (Kc) as follows (Allen *et al.*, 1998):

. $ET_C = K_C \times ET_O$…..40

Where: ETc crop evapotranspiration (mm d-1) which is computed using the CROPWAT8.0 software, Kc crop coefficient (dimensionless) take from different literatures for different crops (FAO56) and ETo reference crop evapotranspiration (mm per day) can be computed using CROPWT8.0 from weather data.

To estimate crop water requirements CROPWAT8 was used. In this study, for the calculation of reference evapotranspiration, FAO (Penman-Monteith) equation is used. To calculate the reference evapotranspiration using FAO (Penman-Monteith) equation, climate data such as minimum and maximum air temperature, relative humidity, sunshine hours and wind speed is required. Other inputs of the model are cultivation pattern, the plant coefficient irrigation scheduling, soil type, the available soil moisture, root depth and water content in the soil.

The coefficient integrates differences in the soil evaporation and crop transpiration rate between the crop and the grass reference surface. As soil evaporation may fluctuate daily as a result of rainfall or irrigation, the single crop coefficient expresses only the time-averaged (multi-day) effects of crop evapotranspiration. The value of K_C is varies for different crop type. The major crops that permanently harvest in Koga Irrigation Project are maize, onion and potato and in this study the water requirement of these three crops was estimated using cropwat8 software. Cropwat8 is a decision support system developed by FAO having which used to calculate reference evapotranspiration, crop water requirement, crop irrigation requirement and develop schedules. The software used maximum and minimum temperature, humidity, wind speed and sunshine for evapotranspiration estimation, and rainfall for effective precipitation computation. To compute crop water requirement of a single crop the software use evapotranspiration, crops, rains and soil as input data that was estimated in cropwat8 from the weather and soil data.

4.5. Estimation of Irrigation Performance Indicators

In this study five irrigation performance indicators were used in order to assess the irrigation performance of the Koga Irrigation Project.

1) Relative water supply

The relative water supply (RWS), used as an indicator of adequacy of irrigation water delivery, compares the amount of the water supply with that of water demand. It is the ratio of total water supply (i.e., irrigation + total rainfall) to total water demand by crop (i.e., potential crop evapotranspiration, ETp). It is computed as:

$$RWS = \frac{V_C + RF}{ET_o} \qquad \text{.....41}$$

Where; Vc is irrigation supply, RF is total rainfall and ETo is potential crop evapotranspiration. The target value of RWS indicator was considered 2.0 (Molden *et al*, 1998).

2) Overall consumed ratio

It is the ratio of irrigation demand (i.e., ETo - effective rainfall) to irrigation supply. The overall consumed ratio quantifies the degree to which crop irrigation requirements are met by irrigation water in the irrigated area. The ratio is defined as.

$$\mathrm{OCR} = \frac{(\mathrm{ET_O} - \mathrm{RF_{eff}})}{\mathrm{V_C}} \qquad \text{.....42}$$

Where; RF_{eff} is effective rainfall. It was calculated in the software CROPWAT8.0. A target overall consumed ratio should be set within an existing irrigated area, and compared to the actual ratio on a monthly and seasonal basis. A value less than or equal to 0.51 can be accepted as the target value at the field level in the conditions of study area (Bastiaanssen *et al*, 2001).

3) Depleted fraction (DF)

The depleted fraction (DF) is the fraction of available water that is depleted and no longer available for other water consumption processes. The depletion in the irrigation scheme is governed by ETc. It is the ratio of actual evapotranspiration (ETc) to total water supply (i.e., irrigation + total rainfall).

$$\mathrm{DF} = \frac{\mathrm{ET_c}}{\mathrm{V_C} + \mathrm{RF}} \qquad \text{.....43}$$

For semi-arid and arid regions, the critical value of the depleted fraction averages about 0.6. The acceptable range of DF was considered 0.6-1.1 (Bastiaanssen *et al*, 2001).

4) Crop water deficit (CWD)

Crop water deficit (CWD) over a period is defined as the difference between ETo and ETc of the cropping pattern within the area. An average CWD of 30 mm per month or 1 mm per day is acceptable. It is defined as follows (Bastiaanssen *et al*, 2001):

$$\mathrm{CWD} = \mathrm{ET_O} - \mathrm{ET_c} \quad \text{.........44}$$

5) Relative evapotranspiration

To evaluate the adequacy of irrigation water delivery to a selected command area as a function of time, the dimensionless ratio of ETc over ETo gives valuable information to the water user manager and is described as relative evapotranspiration (RET). It is a ratio of ETc to ETo.

$$\mathrm{RET} = \frac{\mathrm{ET_c}}{\mathrm{ET_O}} \quad \text{.........45}$$

A value of RET $\geq$ 0.75 is quite acceptable for irrigated agriculture in the growing season, although this is not constant over time (Molden *et al*, 1998).

Table 3.6: Values of ETc, ETo, Vc, RF and RFeff for Koga irrigation project at the satellite over pass time

Month	ET_a	ET_o	ET_c	RF	RF_{eff}	V_C
January 22	0.778	2.98	2.18	0	0	3.49
February 7	0.885	3.39	2.37	0	0	6.586
March 23	1.01	3.37	3.18	1.3	1.2	6.63
April 27	0.997	3.82	4.14	0.6	0.6	6.08
May 29	1.0	3.86	4.3	2.35	2.3	5.79

Note: the source of Irrigation supply (VC) is Koga Irrigation project management office at Koga Merawi.

ETa, ETC, RF, RFeff, Vc and ET_O are the estimated value of actual evapotranspiration, crop water requirement (crop evapotranspiration), rain fall, effective rain fall irrigation supply and potential evapotranspiration of the area respectively.

Table 3.7: Values of OCR, RWS, DF, CWD, and RET for Koga irrigation project

Month	RWS	OCR	DF	CWD	RET
January	1.17	0.85	0.23	2.2	0.26
February	1.94	0.51	0.07	2.9	0.14
March	2.35	0.61	0.003	3.2	0.006
April	1.74	0.52	0.004	3.8	0.007
May	2.09	0.26	0.02	3.7	0.03
Average	1.85	0.55	0.07	3.18	0.09
Acceptable value	2.0	0.51	0.6 – 1.1	>=1	>= 0.75

The values of the ETa, ETc, ETo, Vc, and RFeff are parameters that have been used to determine irrigation performance indicators (Table 3.6). Performance indicators for the evaluation of the irrigation performance are relative water supply (RWS), overall consumed ratio (OCR), depleted fraction (DF), crop water deficit (CWD), and relative evapotranspiration (RET) which have average value of 1.85, 0.49, 0.07, 3.18, and 0.09 respectively (Table 3.7).

CHAPTER FOUR

4. RESULTS AND DISCUSSION

4.1. Estimated Evapotranspiration

4.1.1. SEBAL derived Actual Evapotranspiration

Results have shown that mean evapotranspiration for January, February, March, April and May were 0.778, 0.885, 1.01, 0.997 and 1.0 mm per day respectively. The farmers prepare their farm lands for harvesting in January at Koga Irrigation Project and it is not covered by any crop in this month. So, transpiration is low in January due to lack of crops and vegetation in the area and evaporation is higher than transpiration because it is generated from the soil. Transpiration gradually increases in the next months.

The average daily ET estimated using SEBAL by Ahmed (2006), on Tatra Mountains Region, were 0.72 mm per day. The evapotranspiration estimation varies from method to method. The daily evapotranspiration estimated by Coulomb *et al (*2001) with SEBAL, Penman and Complementary Relationship Evaporation (CRE) methods were 1.777, 1.875 and 1.728 mm respectively. According to Ayenew (2003) estimated evapotranspiration with the SEBS, Penman and SEBAL model have been 2.022, 1.599 and 1.769 mm respectively. So, Evapotranspiration estimated by SEBAL method was more closed to the above listed findings by other researchers at different geographic location. Figure 4.1 below show the spatial distribution of evapotranspiration at Koga Irrigation Project for each month at the satellite overpass time.

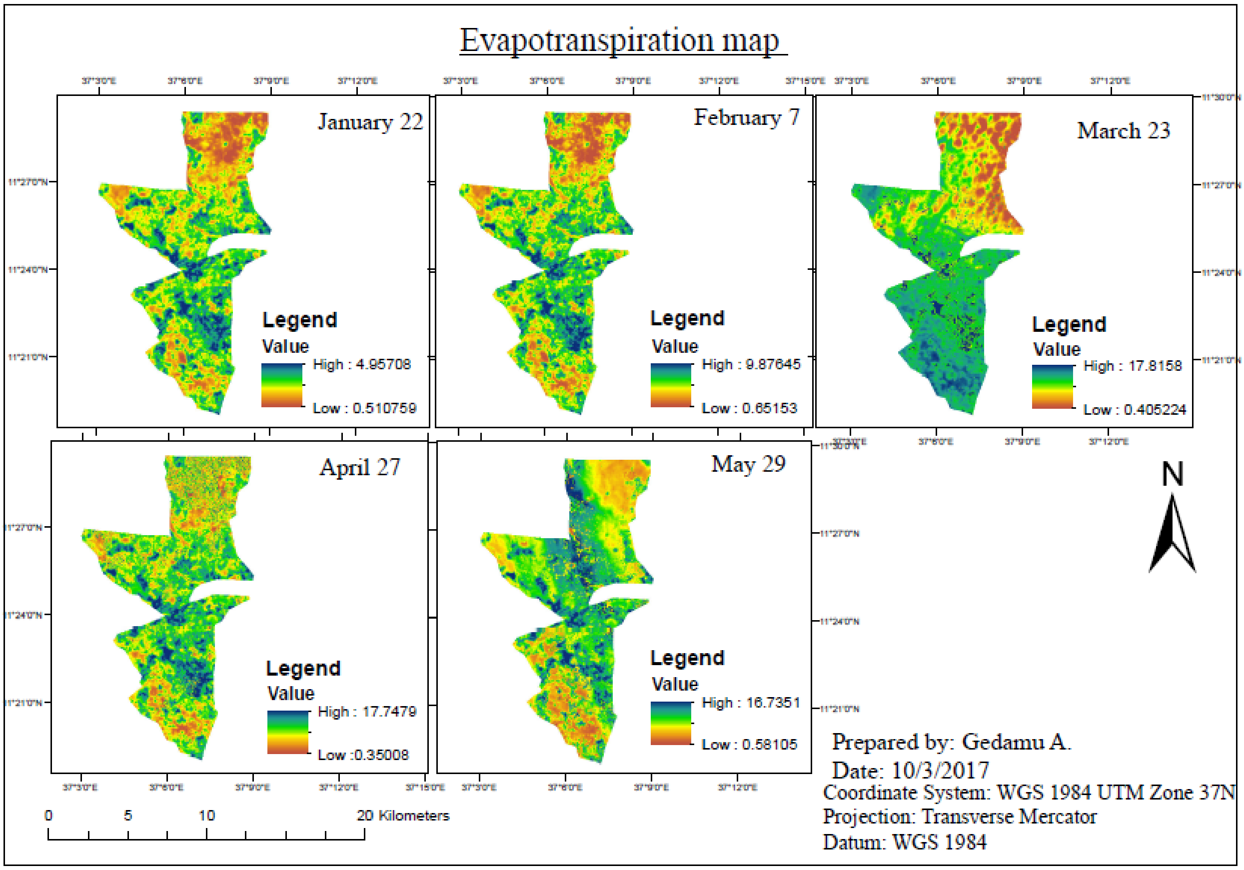

Figure 4.1: Evapotranspiration time series map by SEBAL model

4.1.2. Estimated Reference Evapotranspiration

The FAO method estimate reference evapotranspiration from weather data based on cropwat8. During the estimation of reference evapotranspiration in this method the weather data was used at the weather station rather than pixel by pixel as we are seen in the SEBAL. The maximum monthly potential evapotranspiration exist in March (Table 4.1) because of dry weather condition in the area.

Table 4.1: Average daily evapotranspiration by Penman-Monteith method

Month	Min Temp °C	Max Temp °C	Humidity %	Wind km/day	Sun hours	Rad MJ/m²/day	ETo mm/day
January	6.7	26.3	51	3	9	20.2	2.98
February	8.5	28.1	43	2	9.6	22.5	3.39
March	12	30.9	41	2	9.1	23.1	3.87
April	12.3	28.5	36	1	8.6	22.8	3.82
May	14.1	26.9	68	6	7.4	20.6	3.86
June	12.8	24.6	66	4	6.1	18.4	3.36
July	13.3	23.8	81	10	4	15.3	2.94
August	13.1	23.4	79	10	4.5	16.3	3.03
September	14.4	24.5	75	11	5.8	18.1	3.32
October	11.7	28.6	64	12	7.8	20.1	3.73
November	6.2	20.3	38	11	6.8	17.3	2.58
December	6.2	27.3	51	3	9.3	20	2.89
Average	10.9	26.1	58	6	7.3	19.6	3.31

4.1.3. Comparison of Evapotranspiration from SEBAL and FAO Method

FAO method estimate reference evapotranspiration from the weather data and the estimated ETo value is similar to potential evapotranspiration. SEBAL model estimate evapotranspiration from the satellite images and its result was actual evapotranspiration (ETa). In these study, as presented in figure 4.2 below, actual evapotranspiration is less than the potential evapotranspiration at each satellite overpass time. These indicate that the estimated ETa values in this study are more reliable because it can be estimated pixel by pixel base. The study shows that the maximum and minimum actual and potential evapotranspiration in the area found in March and January indicates that at the planting stage evapotranspiration was minimum and at mid stage it can be maximum and can be reduce at the harvesting stage of the crop.

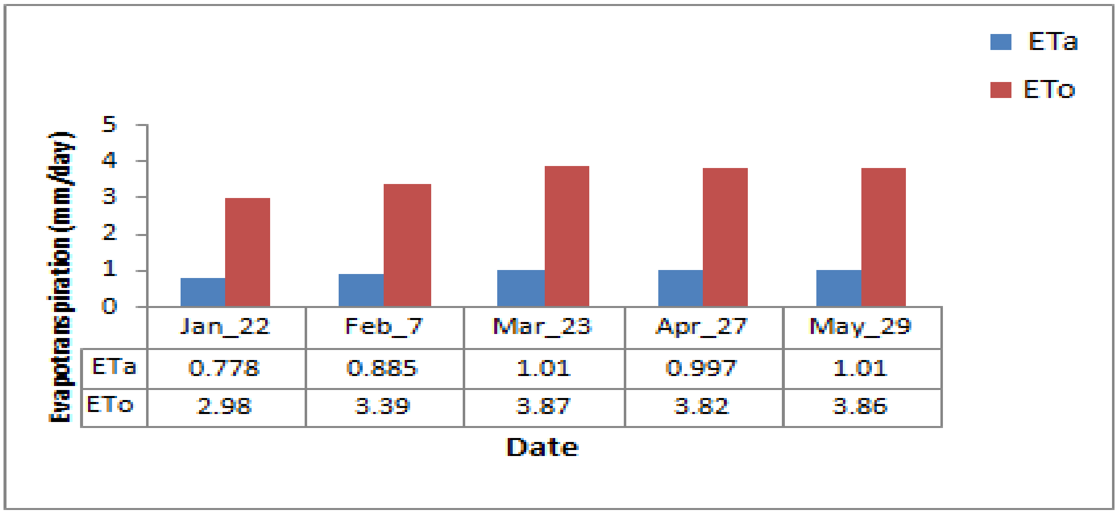

Figure 4.2: comparative analysis of ETa and ETo at the satellite over pass time (mm/day)

4.2. Crop Water Requirement and Irrigation Schedule of Major Crops in the Area

4.2.1. Crop Water Requirement for Maize

In Koga Irrigation project Maize are most dominantly harvested crops. It covers larger areas in irrigated season compared to other crops. But the water consumption of Maize are not estimated, farmers consumed water traditionally depend on the availability of water. As we are seen in the table 16, crop water requirement is equal to Irrigation water requirement particularly in the initial stage because there is no rainfall in this time. As crop growth the leaf of the crop also increase and transpiration is increase gradually. Due to this Irrigation requirement is lower than crop water requirement as crops growing stage increase because of increasing evapotranspiration. Maize needs a total of 611.8 and 597.9 mm/dec of crop water requirement and irrigation requirement respectively within 6 months from the planting date up to the harvesting date. The difference between crop water requirement and irrigation requirement are covered by rainfall. The following tables 4.2 clearly show the crop water requirement and irrigation requirement of maize in area at different stages like initial stage, development stage, mid and later stages of the crop.

Table 4.2: Crop water requirement of Maize

Month	Decade	Stage	Kc Coeff	ETc mm/day	ETc mm/dec	Eff rain mm/dec	IR. mm/dec
Jan	1	I	0.7	2.07	20.7	0	20.7
Jan	2	I	0.7	2.09	20.9	0	20.9
Jan	3	D	0.7	2.19	24	0	24
Feb	1	D	0.76	2.47	24.7	0	24.7
Feb	2	D	0.85	2.88	28.8	0	28.8
Feb	3	D	0.93	3.3	26.4	0.1	26.3
Mar	1	D	1.01	3.75	37.5	0.3	37.2
Mar	2	D	1.1	4.27	42.7	0.5	42.2
Mar	3	M	1.15	4.44	48.8	0.4	48.4
Apr	1	M	1.15	4.42	44.2	0.1	44
Apr	2	M	1.15	4.4	44	0	44
Apr	3	M	1.15	4.41	44.1	0.6	43.6
May	1	M	1.15	4.43	44.3	1.6	42.7
May	2	M	1.15	4.45	44.5	2.4	42.1
May	3	L	1.06	3.91	43	2.2	40.8
Jun	1	L	0.89	3.15	31.5	1.7	29.8
Jun	2	L	0.74	2.47	24.7	1.5	23.2
Jun	3	L	0.59	1.89	17	2.2	14.6
Total					611.8	13.7	597.9

Where, I = Initial Stage, D = Development Stage, M = Mid- Season Stage, L = Late Season Stage, Kc = Crop coefficient, ETc = Crop Evapotranspiration, IR = Irrigation Requirement

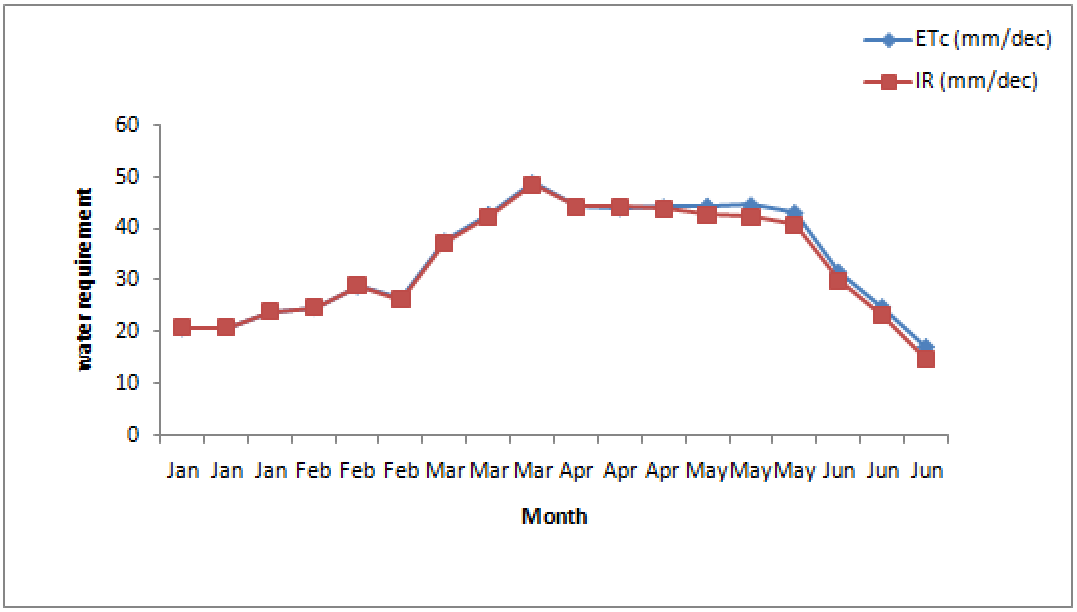

Figure 4.3: Crop water requirement and irrigation requirement of Maize (mm)

4.2.2. Irrigation Schedule of Maize

In the irrigation season at Koga Maize planting in January and harvesting in Jun that means it takes 6 months. It takes 175 days to harvest from initial to the end days. The net irrigation requirement, depletion of moisture from the total available moisture and other related parameters at each stage has been shown (Table 4.3). In the schedule the net irrigation increase as days increases because of the crops water consumption increase.

From the present study it is clear that a planting-window after 4 January can be safely considered for maize planting. The study also indicates that it is not advisable to go for maize planting after December. Proper timing of maize planting is important to achieve higher water use efficiency. Detailed field experiments are necessary to assess the effect of planting dates on maize yield and water use efficiency, keeping the present study as a base.

Table 4.3: Irrigation schedule of Maize

Date	Day	Stage	Rain Mm	Ks fract.	Eta %	Depl %	Net Irr Mm	Deficit Mm	Loss Mm	Gr. Irr Mm	Flow l/s/ha
4-Jan	4	Init	0	1	100	24	8.3	0	0	11.8	0.34
8-Jan	8	Init	0	1	100	21	8.3	0	0	11.8	0.34
13-Jan	13	Init	0	1	100	23	10.4	0	0	14.9	0.34
18-Jan	18	Init	0	1	100	21	10.4	0	0	14.9	0.35
24-Jan	24	Init	0	1	100	23	12.9	0	0	18.5	0.36
30-Jan	30	Init	0	1	100	21	13.1	0	0	18.7	0.36
6-Feb	37	Dev	0	1	100	24	17	0	0	24.3	0.4
13-Feb	44	Dev	0	1	100	23	18.5	0	0	26.4	0.44
21-Feb	52	Dev	0	1	100	27	23.5	0	0	33.5	0.48
1-Mar	60	Dev	0	1	100	27	26.7	0	0	38.2	0.55
9-Mar	68	Dev	0	1	100	28	29.7	0	0	42.5	0.61
18-Mar	77	Dev	0	1	100	32	37.4	0	0	53.4	0.69
27-Mar	86	Mid	0.2	1	100	33	39.2	0	0	56	0.72
5-Apr	95	Mid	0	1	100	33	39.8	0	0	56.8	0.73
14-Apr	104	Mid	0	1	100	33	39.6	0	0	56.6	0.73
23-Apr	113	Mid	0.3	1	100	33	39.4	0	0	56.2	0.72
2-May	122	Mid	0	1	100	33	39.5	0	0	56.4	0.73
11-May	131	Mid	0	1	100	33	39.1	0	0	55.8	0.72
20-May	140	Mid	0	1	100	31	37.6	0	0	53.8	0.69
31-May	151	End	0	1	100	34	40.7	0	0	58.2	0.61
17-Jun	168	End	0.8	1	100	38	45.5	0	0	65	0.44
29-Jun	End	End	0	1	0	17					

The total available moisture (TAM) increase gradually from the plating date up to 80 days and almost it is constant to the harvesting date (Figure 19). The total available moisture, readily available moisture and depletion of moisture in the irrigation schedule of Onion at soil water retention.

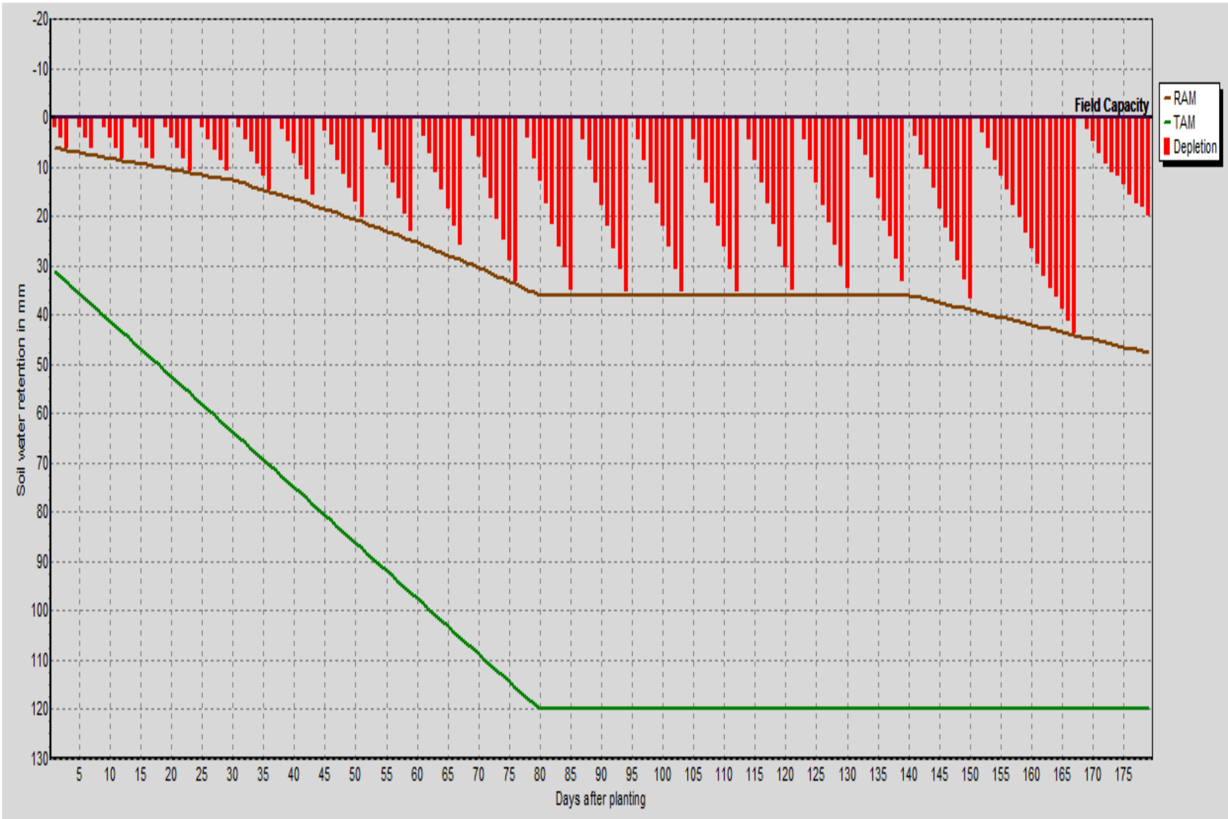

Figure 4.4: Soil water retention of Maize

4.2.3. Crop Water Requirement for Potato

It covers larger area in irrigated season next to Maize and most farmers harvest it. But the water consumption of Potato are not estimated, farmers consumed water traditionally depend on the availability of water. As it has been noticed (Table 4.4) that crop water requirement is equal to Irrigation water requirement especially in the initial stage because it is the perfect time of the Potato planting and there is no rainfall at that stage. As the Potato grows, its leaf also increases and transpiration and water consumption is increase gradually. Due to this Irrigation requirement is lower than crop water requirement as crops growing stage increase because of increasing evapotranspiration and there is also small amount of rainfall. It required a total amount of 428.6 and 418.6 mm/dec crop water requirement and irrigation requirement respectively. The difference between crop water requirement and irrigation requirement are covered by rainfall. It

(Table 4.4) clearly shows the crop water requirement and irrigation requirement of Potato in the area at different stages like initial, development, mid and later stages of the crop.

Table 4.4: Crop water requirement of Potato

Month	Decade	Stage	Kc Coeff	Etc mm/day	ETc mm/dec	Eff rain mm/dec	IR mm/dec
Jan	3	I	0.5	1.56	3.1	0	3.1
Feb	1	I	0.5	1.63	16.3	0	16.3
Feb	2	I	0.5	1.69	16.9	0	16.9
Feb	3	D	0.54	1.91	15.3	0.1	15.2
Mar	1	D	0.72	2.66	26.6	0.3	26.3
Mar	2	D	0.92	3.57	35.7	0.5	35.2
Mar	3	M	1.1	4.24	46.6	0.4	46.2
Apr	1	M	1.12	4.29	42.9	0.1	42.8
Apr	2	M	1.12	4.27	42.7	0	42.7
Apr	3	M	1.12	4.29	42.9	0.6	42.3
May	1	L	1.12	4.3	43	1.6	41.3
May	2	L	1.03	3.97	39.7	2.4	37.3
May	3	L	0.88	3.25	35.8	2.2	33.6
Jun	1	L	0.75	2.64	21.1	1.4	19.4
Total					428.6	9.6	418.6

Where: I = Initial Stage, D = Development Stage, M = Mid- Season Stage, L = Late Season Stage, Kc = Crop coefficient, ETc = Crop Evapotranspiration, IR = Irrigation Requirement

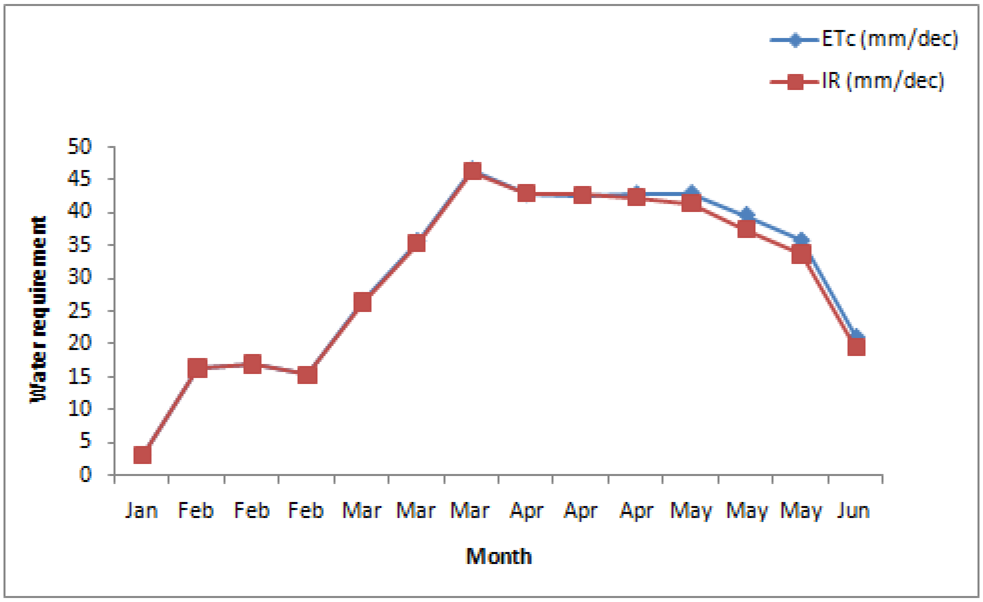

Figure 4.5: Crop water requirement and irrigation requirement of Potato (mm)

4.2.4. Irrigation Schedule of Potato

In the irrigation season at Koga irrigation project Potato planting in February and harvesting in the beginning of June, takes 4 months (125 days) to harvest from initial to the end days. The net irrigation requirement, depletion of moisture from the total available moisture and other related parameters at each stage and in the schedule the net irrigation increase as days increase because of the crops water consumption increase (Table 4.5).

Table 4.5: Irrigation schedule of Potato

Date	Day	Stage	Rain Mm	Ks fract.	Eta %	Depl %	Net Irr Mm	Deficit Mm	Loss	Gr. Irr Mm	Flow l/s/ha
5-Feb	7	Init	0	1	100	22	11.3	0	0	16.1	0.27
12-Feb	14	Init	0	1	100	20	11.5	0	0	16.5	0.27
20-Feb	22	Init	0	1	100	22	13.6	0	0	19.4	0.28
28-Feb	30	Dev	0	1	100	22	15.2	0	0	21.6	0.31
7-Mar	37	Dev	0.2	1	100	24	18.3	0	0	26.1	0.43
14-Mar	44	Dev	0	1	100	27	22	0	0	31.5	0.52
21-Mar	51	Dev	0	1	100	29	25.4	0	0	36.3	0.6
28-Mar	58	Mid	0	1	100	33	29.3	0	0	41.8	0.69
4-Apr	65	Mid	0	1	100	33	29.8	0	0	42.6	0.7
11-Apr	72	Mid	0	1	100	33	29.9	0	0	42.8	0.71
18-Apr	79	Mid	0	1	100	33	29.9	0	0	42.7	0.71
25-Apr	86	Mid	0	1	100	33	29.7	0	0	42.4	0.7
2-May	93	Mid	0	1	100	33	29.7	0	0	42.5	0.7
9-May	100	Mid	0	1	100	33	29.3	0	0	41.8	0.69
17-May	108	End	1.2	1	100	33	29.7	0	0	42.4	0.61
27-May	118	End	1.1	1	100	36	32.5	0	0	46.4	0.54
8-Jun	End	End	0	1	0	33					

The figure 4.6 shows that the total available moisture, readily available moisture and depletion of moisture in the irrigation schedule of Potato at soil water retention.

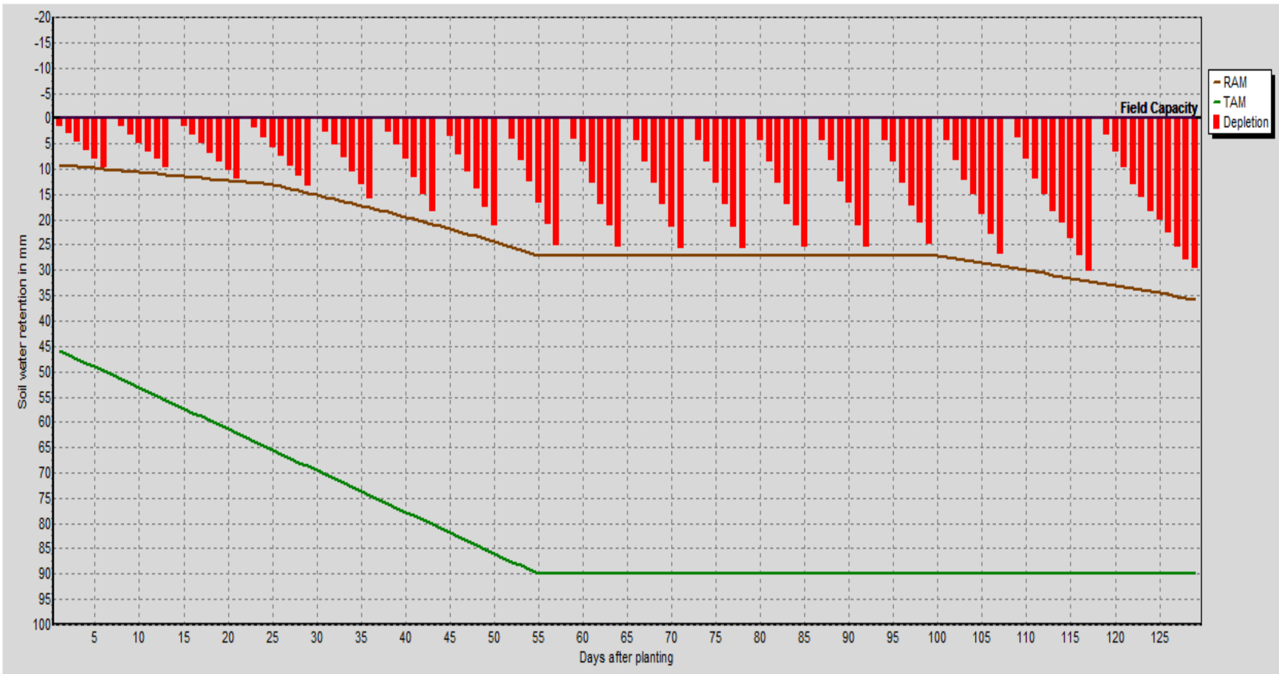

Figure 4.6: Soil water retention of Potato

4.2.5. Crop Water Requirement for Onion

In Koga Irrigation project Onion is also more commonly harvested vegetation by farmers next to Potato. It covers larger area in irrigated season and most farmers harvest it. But the water consumption of Onion has not been estimated and farmers consumed water traditionally depends on the availability of water. As it can be analyzed that crop water requirement is equal to Irrigation water requirement especially in the initial stage because it is almost at the planting stage and have low transpiration. As it growth its leafe develop its water consumption and transpiration is increase gradually. Du to this Irrigation requirement is lower than crop water requirement as crops growing stage increase because of increasing evapotranspiration. It needs a total of 428.6 and 418.6 mm/dec of crop water requirement and irrigation requirement respectively within 4 months from the planting date up to the harvesting date. The difference between crop water requirement and irrigation requirement are covered by rainfall. The following table 4.6 clearly shows the crop water requirement and irrigation requirement of Onion in the area at different stages like initial, development, mid and later stages of the crop.

Table 4.6: Crop water requirement of Onion

Month	Decade	Stage	Kc Coeff	ETc mm/day	ETc mm/dec	Eff rain mm/dec	IR mm/dec
Jan	3	I	0.5	1.56	3.1	0	3.1
Feb	1	I	0.5	1.63	16.3	0	16.3
Feb	2	I	0.5	1.69	16.9	0	16.9
Feb	3	D	0.54	1.91	15.3	0.1	15.2
Mar	1	D	0.72	2.66	26.6	0.3	26.3
Mar	2	D	0.92	3.57	35.7	0.5	35.2
Mar	3	M	1.1	4.24	46.6	0.4	46.2
Apr	1	M	1.12	4.29	42.9	0.1	42.8
Apr	2	M	1.12	4.27	42.7	0	42.7
Apr	3	M	1.12	4.29	42.9	0.6	42.3
May	1	L	1.12	4.3	43	1.6	41.3
May	2	L	1.03	3.97	39.7	2.4	37.3
May	3	L	0.88	3.25	35.8	2.2	33.6
Jun	1	L	0.75	2.64	21.1	1.4	19.4
Total					428.6	9.6	418.6

Where: I = Initial Stage, D = Development Stage, M = Mid- Season Stage, L = Late Season Stage, Kc = Crop coefficient, ETc = Crop Evapotranspiration, IR = Irrigation Requirement

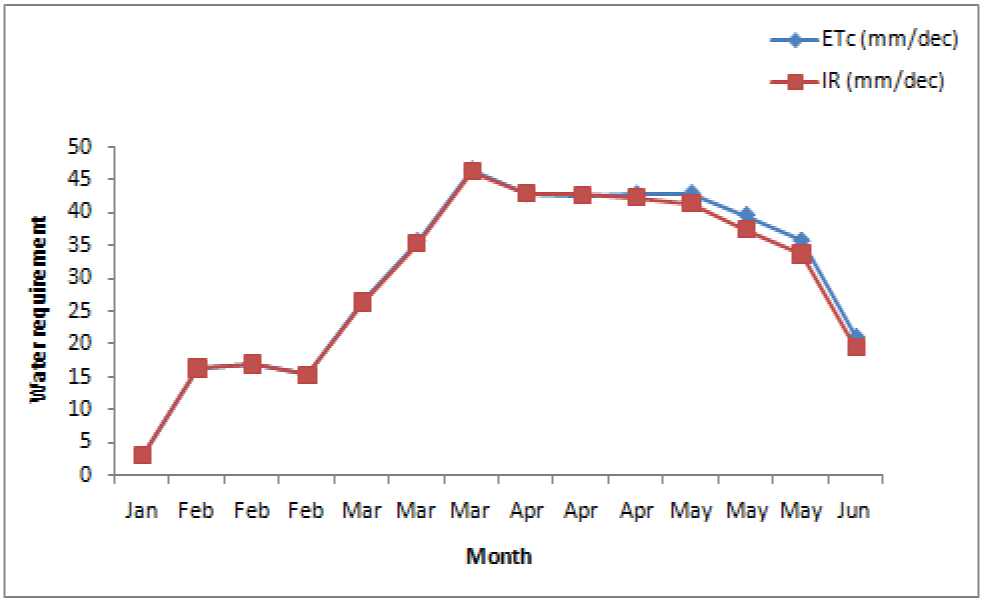

Figure 4.7: Crop water requirement and irrigation water requirement of Onion (mm)

4.2.6. Irrigation Schedule of Onion

In the irrigation season at Koga Onion planting at the end of January and harvesting at the beginning of Jun that means it takes 4 months. It takes 125 days to harvest from initial to the end days. The following table 4.7 shows the net irrigation requirement, depletion of moisture from the total available moisture and other related parameters at each stage and in the schedule the net irrigation increase as days increase because of the crops water consumption increase.

Table 4.7: Irrigation schedule of Onion

Date	Day	Stage	Rain Mm	Ks fract.	Eta %	Depl %	Net Irr Mm	Deficit Mm	Loss Mm	Gr. Irr Mm	Flow l/s/ha
5-Feb	7	Init	0	1	100	22	11.3	0	0	16.1	0.27
12-Feb	14	Init	0	1	100	20	11.5	0	0	16.5	0.27
20-Feb	22	Init	0	1	100	22	13.6	0	0	19.4	0.28
28-Feb	30	Dev	0	1	100	22	15.2	0	0	21.6	0.31
7-Mar	37	Dev	0.2	1	100	24	18.3	0	0	26.1	0.43
14-Mar	44	Dev	0	1	100	27	22	0	0	31.5	0.52
21-Mar	51	Dev	0	1	100	29	25.4	0	0	36.3	0.6
28-Mar	58	Mid	0	1	100	33	29.3	0	0	41.8	0.69
4-Apr	65	Mid	0	1	100	33	29.8	0	0	42.6	0.7
11-Apr	72	Mid	0	1	100	33	29.9	0	0	42.8	0.71
18-Apr	79	Mid	0	1	100	33	29.9	0	0	42.7	0.71
25-Apr	86	Mid	0	1	100	33	29.7	0	0	42.4	0.7
2-May	93	Mid	0	1	100	33	29.7	0	0	42.5	0.7
9-May	100	Mid	0	1	100	33	29.3	0	0	41.8	0.69
17-May	108	End	1.2	1	100	33	29.7	0	0	42.4	0.61
27-May	118	End	1.1	1	100	36	32.5	0	0	46.4	0.54
8-Jun	End	End	0	1	100	33					

The figure 4.8 below shows that the total available moisture (TAM), readily available moisture (RAM) and depletion of moisture in the irrigation schedule of Onion at soil water retention.

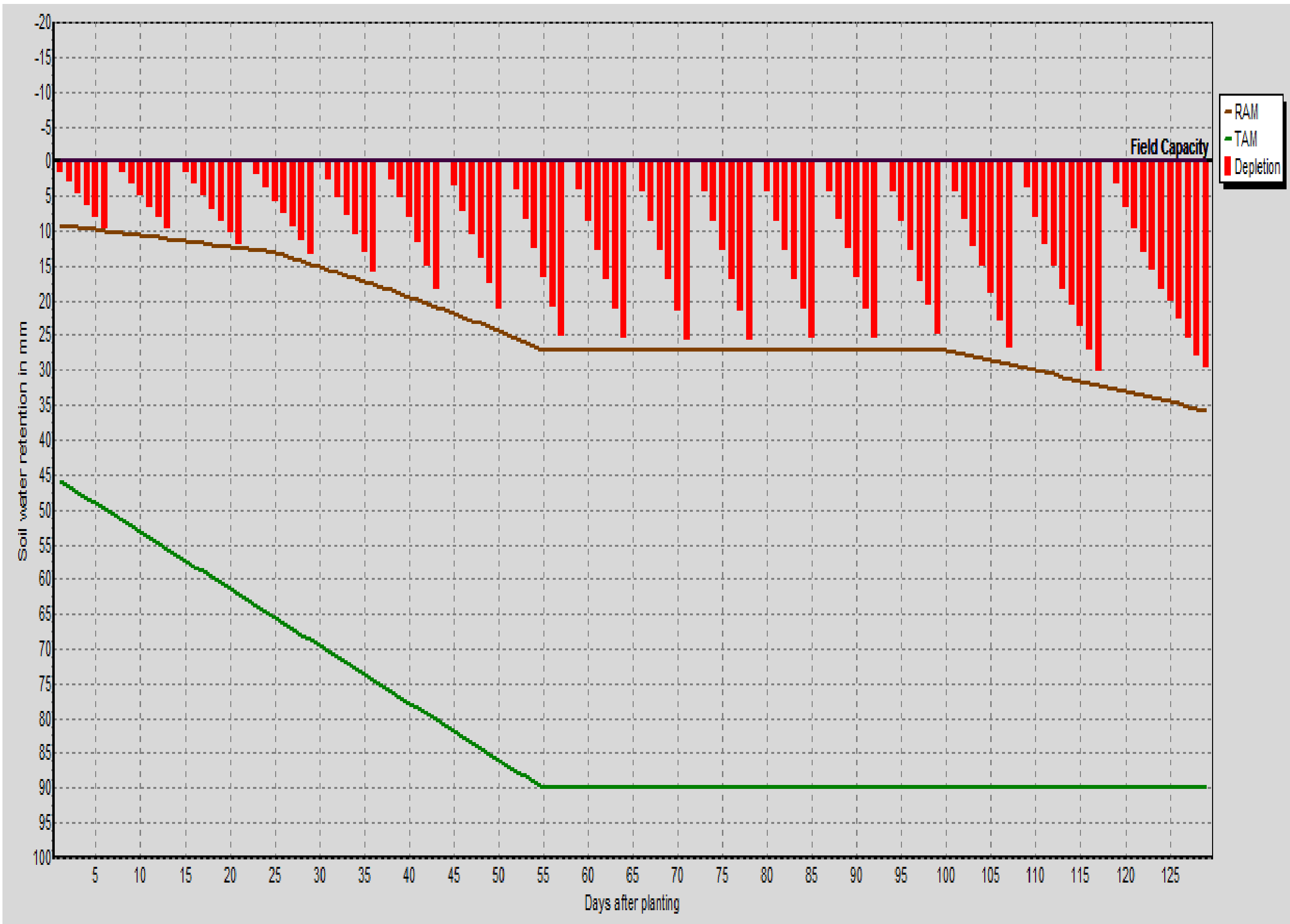

Figure 4.8: Soil water retention of Onion

Readily available water (RAW) is the water that a plant can easily extract from the soil. RAW is the soil moisture held between field capacity and a nominated refill point for unrestricted growth. In this range of soil moisture, plants are neither waterlogged nor water-stressed. Plant roots will continue to take water from the soil after the refill point is reached, but this water is not as readily available and the crop finds it difficult to extract. If the soil dries to the permanent wilting point, the plant can no longer remove any water from it: some water may still be present but is completely unavailable. The drier the soil, as shown by high tensiometer values, the more water needs to be added to bring the soil back to field capacity.

4.3. Irrigation Performance Assessment

Performance assessment is the systematic observation, documentation and interpretation of the management of an irrigation and drainage system to ensure intended outputs and proper functioning. Strategic performance of irrigation is assessed considering the water balance components which derived from satellite images and weather dates, using indicators selected in Table 7. LANDSAT8 image was taken for assessing irrigation performance during the dry season of January to May 2016 in the study area. The values of ETa derived from the satellite measurements were combined with the field measurements. To estimate ET, daily weather data was associated with the satellite measurements. The major source of water in Koga Irrigation Project is rivers and ground waters stored in the Koga dame. The way of living of the people in the Koga and the surrounding areas can greatly improve and the output from the production shall contribute to the general economy of the area if the water source is utilized for irrigation in proper manner as per the water requirement of the crop. The performance of Koga Irrigation Project was asses using the following performance assessment indicators which are governed by its acceptable values. The values of each indicator are determined in Table 7 above.

The parameters for the estimation of the irrigation performance indicators of the Koga irrigation areas were presented in the table 6 above, likewise, the indicators for estimating irrigation performance were also presented in the table 7 above. In cases of water logging and salinity, the critical groundwater depth is mostly dependent on the effective rooting depth of the crop, the overall consumed ratio of irrigation water use and the hydraulic characteristics of the unsaturated soil (Bos *et al*., 2005). When the ratios are low, the non-consumed fraction of the water will cause the groundwater table to rise (Bos *et al*., 1991), while during the periods with high ratios; groundwater must be pumped and stored to avoid water shortage.

In 2016/2017 irrigation period, the average Overall Consumed Ratios in the area was 0.55, which are greater than the target value, indicating that less water was supplied to the field than the demand of the crops. The amount of water supplied to the field was much higher in March than the other months (Table 3.6), because the dry season was at its peak point and the water consumption of crop increase in March and substantial amount of water was needed to meet the crop water requirement.

The relative water supply (RWS) is a basic indicator that informs the irrigation managers of under-supply as well as over- supply in the field (Wolters, 1992). This does not explain the degree of water scarcity in the crop because it does not take into account the groundwater supply (Bastiassen, 2001). For further analysis, the relative evapotranspiration takes the groundwater into account. There is a negative relationship between OCR and RWS (Bastiassen, 2001). The average RWS of Koga irrigation project was found to be 1.85 (Table 3.7), which was less than the target value of 2.0, study done by Molden *et al* (1998) indicates that the water supply was less as compared with the demand in the area. The value of DF and RET in the area were 0.07 and 0.09 which shows that its value do not confirmed to the target values of 0.6 and 0.75 respectively and indicates that there was poor delivery of water in the irrigation area. The average value of CWD was 3.18 which was not confirms to the target values of 1mm/day indicates that the irrigation project were not perform well which have the same diction like the other indicators. According to Molla (2009) study at Kobo irrigation project, the value of OCR, RWS, DF, CWD and RET were 0.55, 1.56, 0.29, 1.41 and 0.43 respectively. These values were more closed with the performance indictor value estimated in this study at Koga irrigation project. The study shows that based on the selected performance indicators Koga irrigation project were not well performed. Because during the fieldwork it was observed that most of the area have broken canals and laterals, and much of the water went into waste and the farmers used water in rotation in the study area. Even though huge amount of water was supplied to the field in these areas which could have affected the crops, but this is not in the case of study area.

For proper irrigation system, the crop water requirements of every crop are normally taken into consideration but this is not still applied in the irrigation system and its Irrigation was normally done on timely basis. Koga Irrigation project has not knowledgeable and capable project engineers and staffs who can manage the system efficiently. Moreover, lack of support from the government has greatly affected the system. The irrigation performance of the Koga irrigation project has not been studied well.

CHAPTER FIVE

5. CONCLUSION AND RECOMMENDATION

5.1. Conclusion

The overall aim of this research was estimation of evapotranspiration by using both SEBAL model and FOA method. The ETa and ETo was estimated in SEBAL model, from LANDSAT8 images, and FAO methods, from weather data, respectively. In this study the mean estimated value of ETa and ETo at the satellite over pass time, on January 22, February 7, March 23, April 27 and May 29, was 0.778, 0.885, 1.0, 0.997 and 1.01 and 2.98, 3.39, 3.87, 3.82 and 3.86 respectively. This shows that in this study actual evapotranspiration is less than the potential evapotranspiration and they have the same pattern. That means as reference evapotranspiration increase actual evapotranspiration also increase and vice versa.

The study has computed crop water requirement and irrigation schedule using cropwat8 software. The water requirement and irrigation schedule of Maize, Potato and Onion was computed from the planting date up to the harvesting date. The results indicate the maximum water requirement of Maize (Table 4.2), Potato (Table 4.4) and onion (Table 4.6) was 48.8, 46.6 and 46.6 mm/day respectively that exist in the middle stage of the crop on March. The water requirement of each crop increases gradually and then decrease when the crop becomes riches at the harvesting stage. The length of harvesting time is different for each crop and also the amount of water consumption was different at different stage.

This research has assessed irrigation performance based on the irrigation performance indicators. The indicators employed in this study was relative water supply, overall consumed ratio, depleted fraction and relative evapotranspiration. Based on these indicators the performance of Koga Irrigation Project was assessed. The overall average estimated value of RWS, OCR, DF, CWD and RET was 1.452, 0.638, 0.458, 24.216 and 0.74 respectively. All indicators have been estimated were not on the range of the standards except CWD that shows the Koga Irrigation project was not well performed upon its final potential. Due to this, the stakeholders on this project were not get maximum value of products and it needs to adjust water consumption of each crop. The water loss through evapotranspiration can be composite by increasing the supply of water.

The irrigation performance of the Koga irrigation project studied was poor. The poor performance is a result of operational and physical deficiencies in the system. Most of the canals and laterals leading to the command areas were broken down and this has become difficult to assess irrigation performance. Data for estimating most of the indicators are missing at the time of visit. There was no data on groundwater supply and this play important role when considering the amount of water supply to the system.

5.2. Recommendation

The application of remote sensing brings a significant contribution to estimate the spatial evapotranspiration in large scale for all types of land covers than ground based estimation of evapotranspiration from weather data. However, the ground observation based methods are always very important, especially in validating the results of different remote sensing based approaches.

Using the natural resource combined with the best irrigation practices is the best way for improving the life of the people. The pressurized irrigation project that is under implementation is one of the development projects that can improve the life of the people. Among this Koga Irrigation Project was the one that are currently implemented to improve the living standards of the surrounding community. Therefore the land that can be irrigated using surface water source could not be much due to limited water resource and emphasis should be given for pressurized irrigation system. No research was done on the irrigation performance of the Koga irrigation system with the help of GIS and Remote Sensing and therefore it is very difficult to get literature on these studies at micro level crop lands. So, depends on this study the researcher recommended on the following points.

- Assure the performance assessment programs for different irrigation project with a minimum number of indicators as they are used in this study and gives brief information for the decision makers, professionals and stakeholders.
- GIS and Remote Sensing based estimation of evapotranspiration is better than ground based estimation of evapotranspiration from the weather data in terms of time and cost.

- Implementing real time weather data measurements to support ETa estimation based on remote sensing methods.
- Organized the Farmers and linking with the experts and give practical implementation of water requirements of each crops and irrigation schedules to chive the performance of irrigation and increase productivity.

Finally the researcher recommends future work about change of land use land cover on the rate of evapotranspiration by focusing on limited time series that can affect the rate and compression of different surface energy balance algorithms to estimate evapotranspiration and irrigation performance assessments.

REFERENCE

Abdo, F., & McCartney, M. (2010). Evaluating the Technical Performance of the Koga and Gomit Reservoirs in the Blue Nile under Existing Conditions and Possible Climate Change. Ethiopia, International Water Management Institute (IWMI).

Ahmed, H. (2016). Estimation of Evapotranspiration Using SEBAL Algorithm and Landsat-8 Data. A Case Study: Tatra Mountains Region. Journal of Geological Resource and Engineering, 5(6), USA.

Akdim, N. (2014). Monitoring of irrigation schemes by remote sensing: phenology versus retrieval of Biophysical variables. Remote sensing (Vol.6).

Allen, R. (1998). Crop evapotranspiration guidelines for computing crop water requirement, FAO irrigation and drainages paper. Rome: Food and Agriculture organization the United Nations, Rome.

Allen, R., Tasumi, M. and Trezza, R. (2002). SEBAL (Surface Energy Balance Algorithms for Land) -Advanced Training and User's Manual-Idaho Implementation, Version 1.0.

Andreas, P., & Karen, F. (2002). Crop Water Requirements and Irrigation Scheduling. Water Resources Development and Management Officers, FAO Sub-Regional Office for East and Southern Africa, Zimbabwe.

Awulachew, S. (2005). Experiences and Opportunities for Promoting Small-Scale/Micro Irrigation and Rainwater Harvesting for Food Security in Ethiopia (No. 98). Colombo, Sri Lanka. Retrieve from http://www.iwmi.cgiar.org/Publications/Working_Papers/working/WOR98.pdf

Ayad, A., Ahmed, H., & Adrian, O., (2016). Estimation of Evapotranspiration Using SEBAL Algorithm and Landsat-8 Data—A Case Study: Tatra Mountains Region. Journal of Geological Resource and Engineering 6, 257-270.

Ayenew, T, 2003. Evapotranspiration Using Thematic Mapper Spectral Satellite Data in the Ethiopian Rift and Adjacent Highlands, Ethiopia: Addis Ababa University.

Ayoub, A. (2008). Decision Support System for Estimating Actual crop Evapotranspiration using Remote Sensing, GIS and Hydrological Models, Malaysia, Kula Lumpur.

Bandara, K.M.P.S. (2006). Assessing irrigation performance by using remote sensing. Doctoral thesis, Wageningen University, Wageningen, The Netherlands.

Bastiaanssen W.G.M. (1995). Regionalization of surface flux densities and moisture indicators in composite terrain. Ph,D Thesis, Wageningen Agricultural University, Wageningen, The Netherlands.

Bastiaanssen W.G.M. (2000). SEBAL-based sensible and latent heat fluxes in the irrigated Gediz Basin, Turkey.

Bastiaanssen W.G.M., and Chandrapala L. (2003). Water balance variability across Sri Lanka for assessing agricultural and environmental water use. Journal of Agricultural water management ISSN: 0378-3774.

Bastiaanssen, W.G.M. (2003). A new crop yield forecasting model based on satellite measurements applied across the Indus Basin, Pakistan. Agriculture, Ecosystems and Environment.

Bastiaanssen, W. (1998). Aremote sensing surface energy balance algorithm for Land (SEBAL), Journal of Hydrology 212–213.

Bastiaanssen, W. (2005). SEBAL model with remotely sensed data to improve water-resources management under actual field conditions. J. Irrig. Drain.

Bos, MG. (1991). The Viejo Retamo secondary canal performance evaluation case study: Mendoza, Argentina. Irrigation and Drainage Systems (5): page 77-88.

Bos, MG. (2005). Irrigation and Drainage Performance Assessment: Practical Guidelines. CABI Publishing. Trowbridge, UK.

Brutsaert, W. (1982). Evaporation into the Atmosphere: Theory, History, and Applications.

CSA (Central Statistical Agency of Ethiopia). (2008). Statistical Abstract of Ethiopia, Central Statistical Agency, Addis Ababa: Ethiopia.

Dessalegn, R. (1999). Water Resource Development in Ethiopia: Issues of Sustainability and Participation. Forum for Social Studies (FFS). Addis Ababa. Ethiopia.

Coulomb, C. (2001). Lake Evapotranspiration Estimates in Tropical Africa (Lake Ziway of Ethiopia*)*.

Hute, A.R. (1988). A soil adjusted vegetation index. Remote sensing of environment, Vol 25 issue 3.

Mekonen, T., & Kebede, F. (2011). Suitability of Koga Watershed for Irrigated Sugarcane and Onion Production in the Blue Nile Basin, Ethiopia.

Ministry of Water Resources (MoWR). (2005). Koga Irrigation Project. Dam Design Report (DRAFT).

Molden P. (1998). Indicators for comparing Performance of Irrigated Agricultural Systems. International Water Management Institute (IWMI), Sri Lanka.

Molla, T. (2009). Estimation of Evapotranspiration for Irrigation Performance Assessment Using Satellite Remote Sensing at Kobo Valley Irrigation Project, Northern Ethiopia.

MoWR (Ministry of Water Resources), (2002). Water Sector Development Program (WSDP), Addis Ababa: Ethiopia.

Othoman, A., Clariza, F., Kenji, J., & Atsushi T. (2006). Comparison of Several Reference Evapotranspiration Methods for Itoshima Peninsula Area, Fukuoka, Japan. Memoirs of the Faculty of Engineering, Kyushu University, Vol. 66(1).

Schell, J. (2000). The developer of normalized differential vegetation index.

Su, Z. The Surface Energy Balance System (SEBS) for estimation of turbulent heat fluxes, ITC, University of Twente Enschede, The Netherlands.

Jia, L. (2003). Estimation of sensible heat flux using the surface energy balance system SEBS and ATSR measurements, ITC, University of Twente Enschede, The Netherlands.

Perry et al, (2009). Increasing productivity in irrigated agriculture Agronomic constraints and hydrological realties.

Wolters W, (1992), Influences on the Efficiency of Irrigation Water Use, International Institute of Land Reclamation and Improvement (ILRI),Wageningen, The Netherlands.

UNESCO (United Nations Educational, Scientific and Cultural Organization), (2004). National development report for Ethiopia, UNESCO, World Water Assessment Program.

X. Zhang, T. (2008). MODIS estimates of heat fluxes: Effect of surface heterogeniety," in Geoscience and Remote Sensing Symposium. IEEE International,.

Appendix

Appendix 1: Normalized Differential Vegetation Index (NDVI)

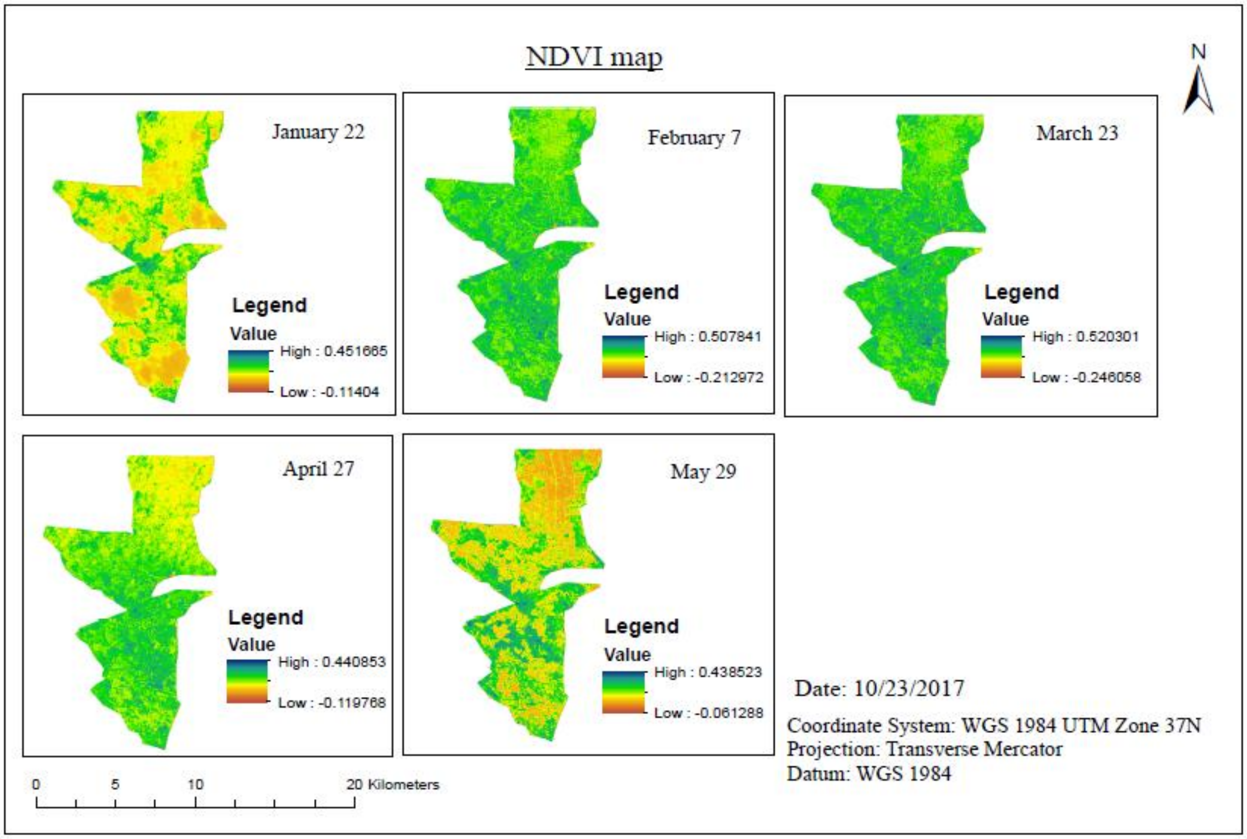

Appendix 2: Soil adjusted Vegetation Index (SAVI)

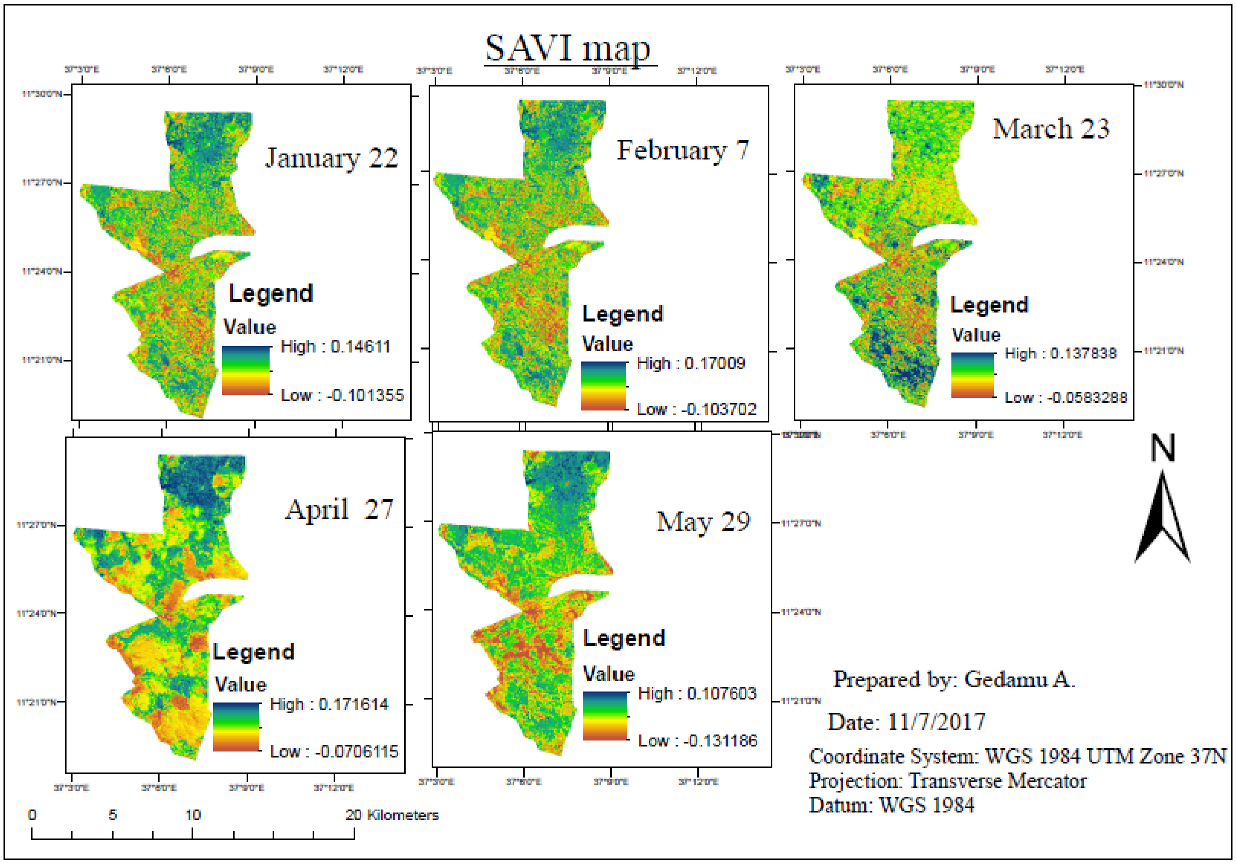

Appendix 3: Leaf Area Index (LAI)

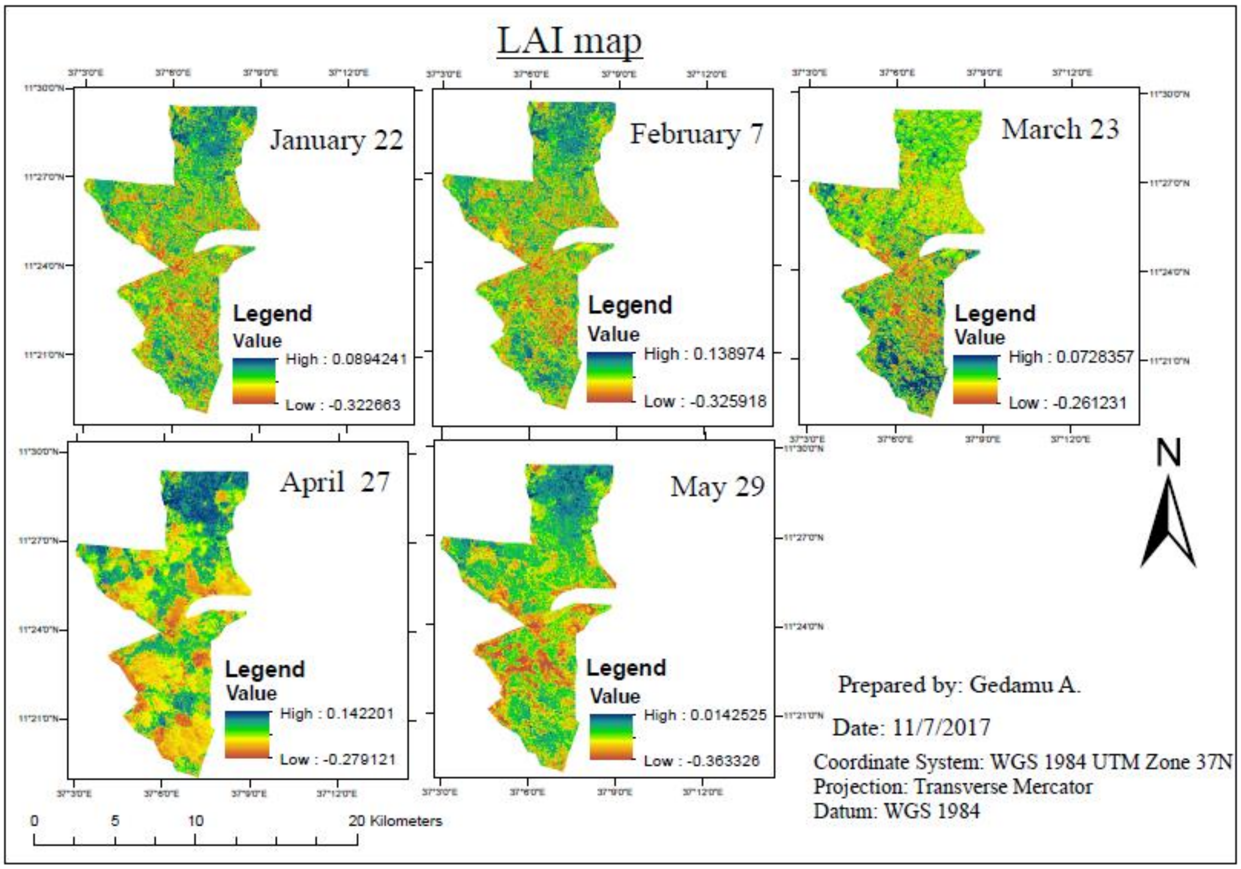

Appendix 4: Surface Emissivity

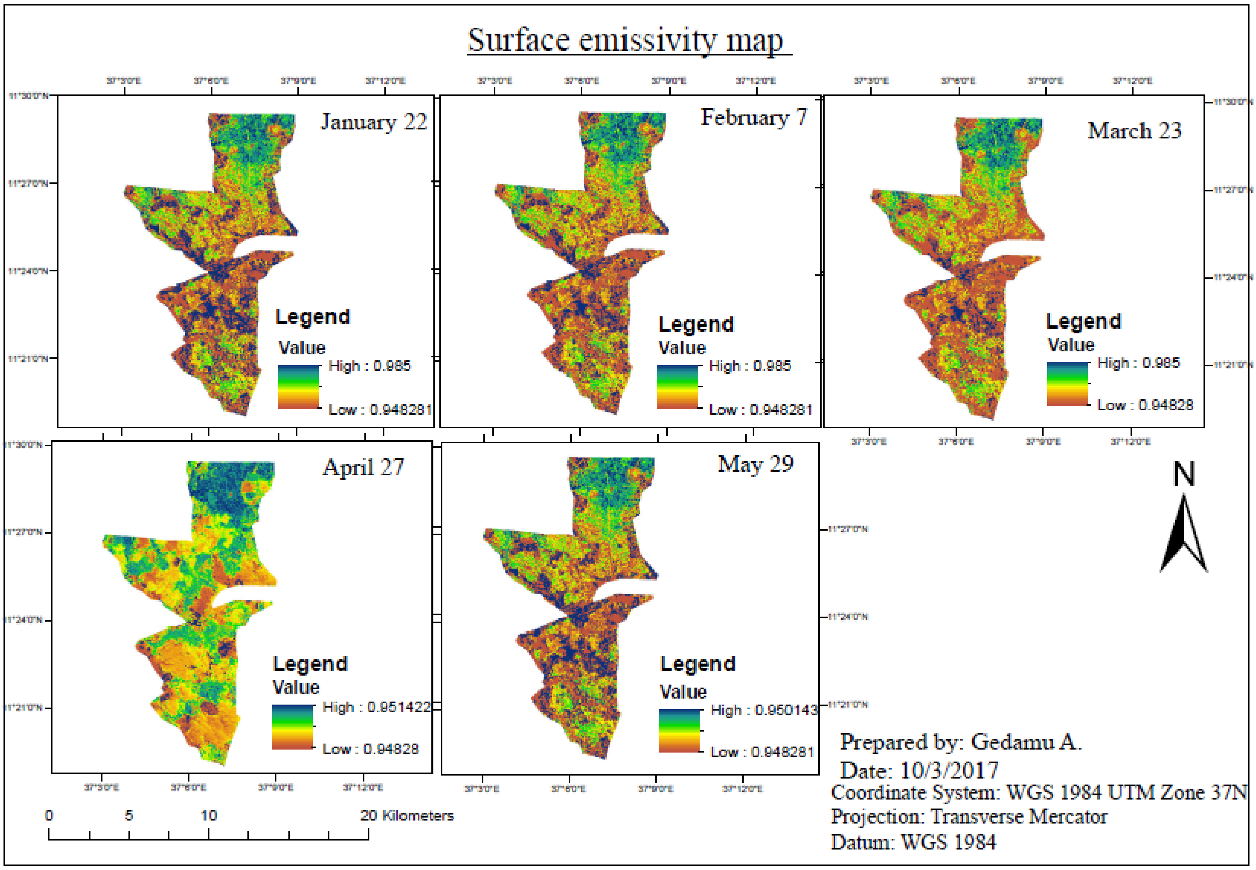

Appendix 5: Net Surface Radiation Flux (Rn)

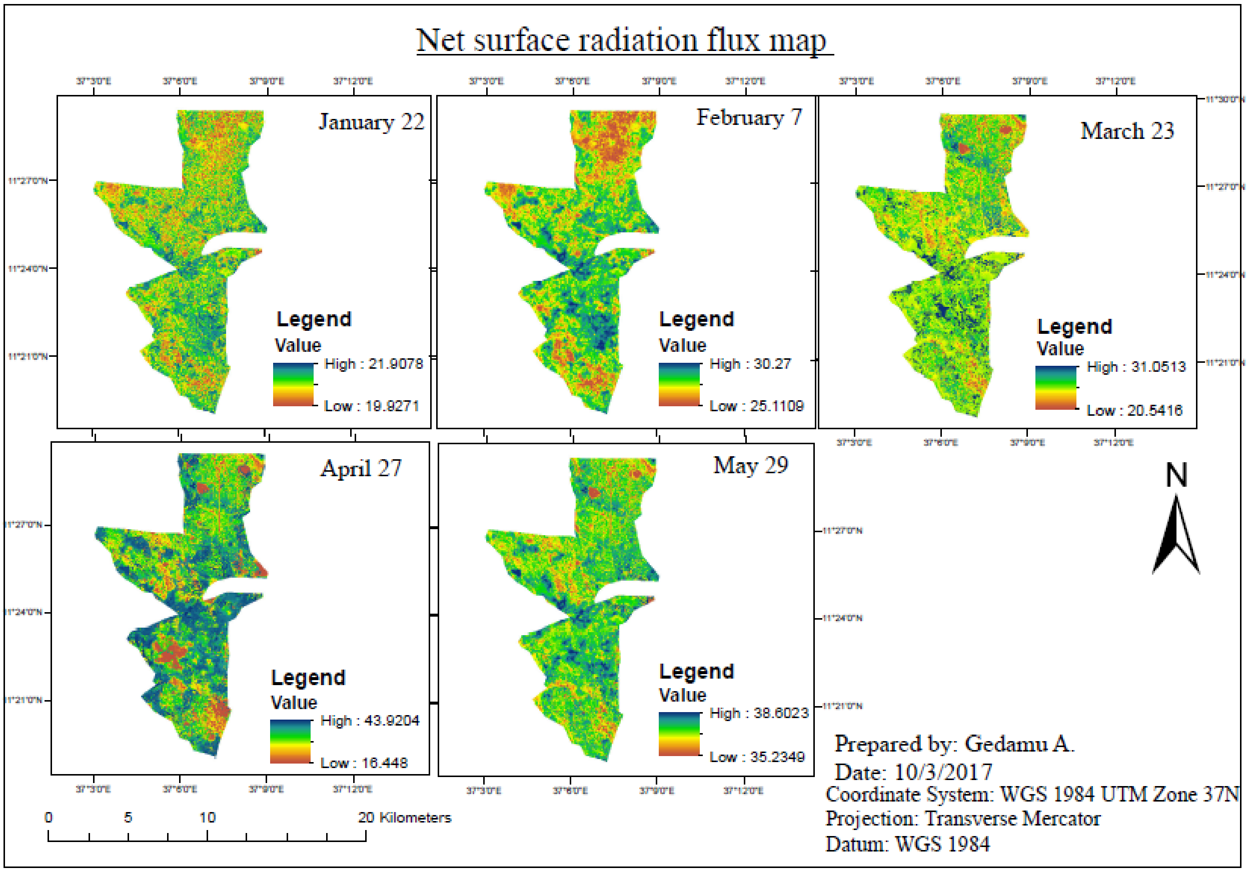

Appendix 6: Soil Heat Flux (G)

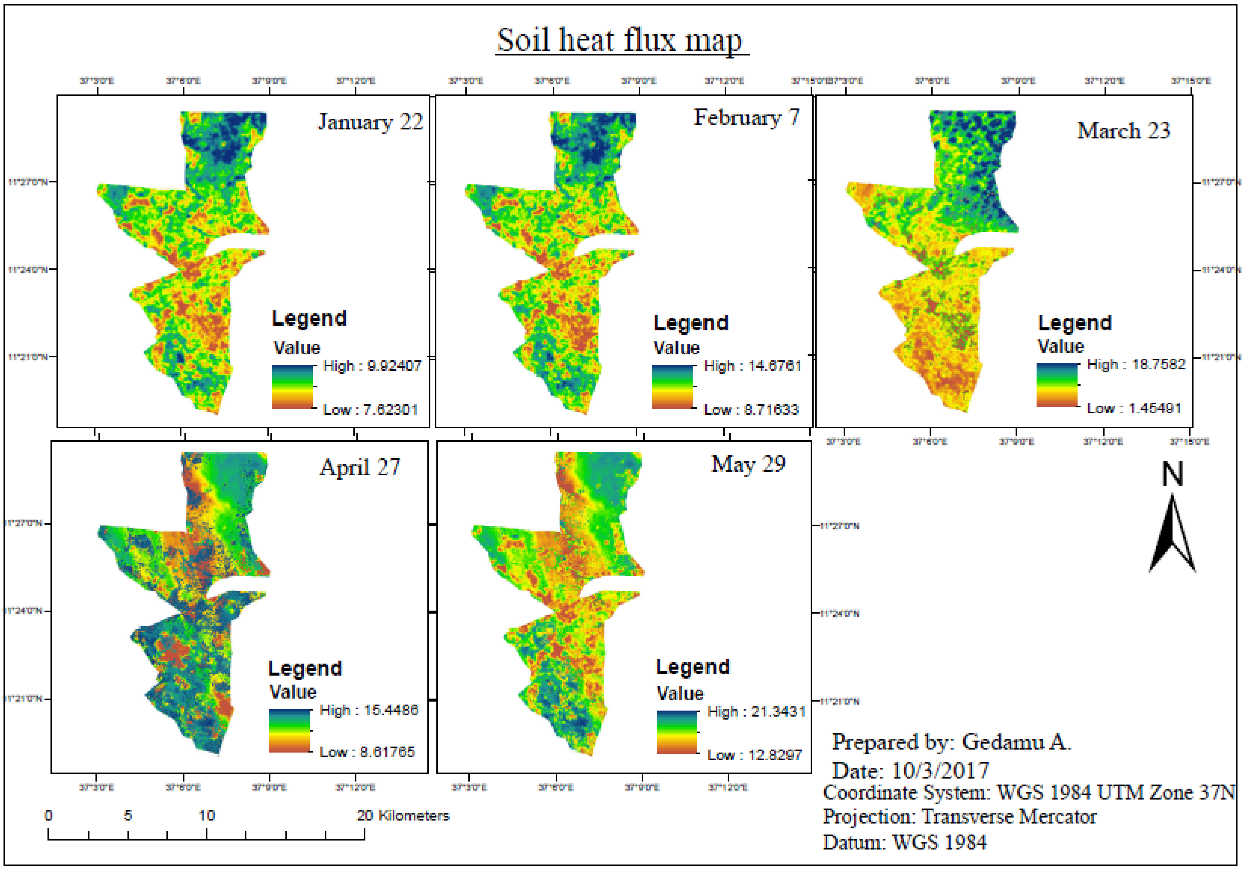

Appendix 7: Sensible Heat Flux (H)

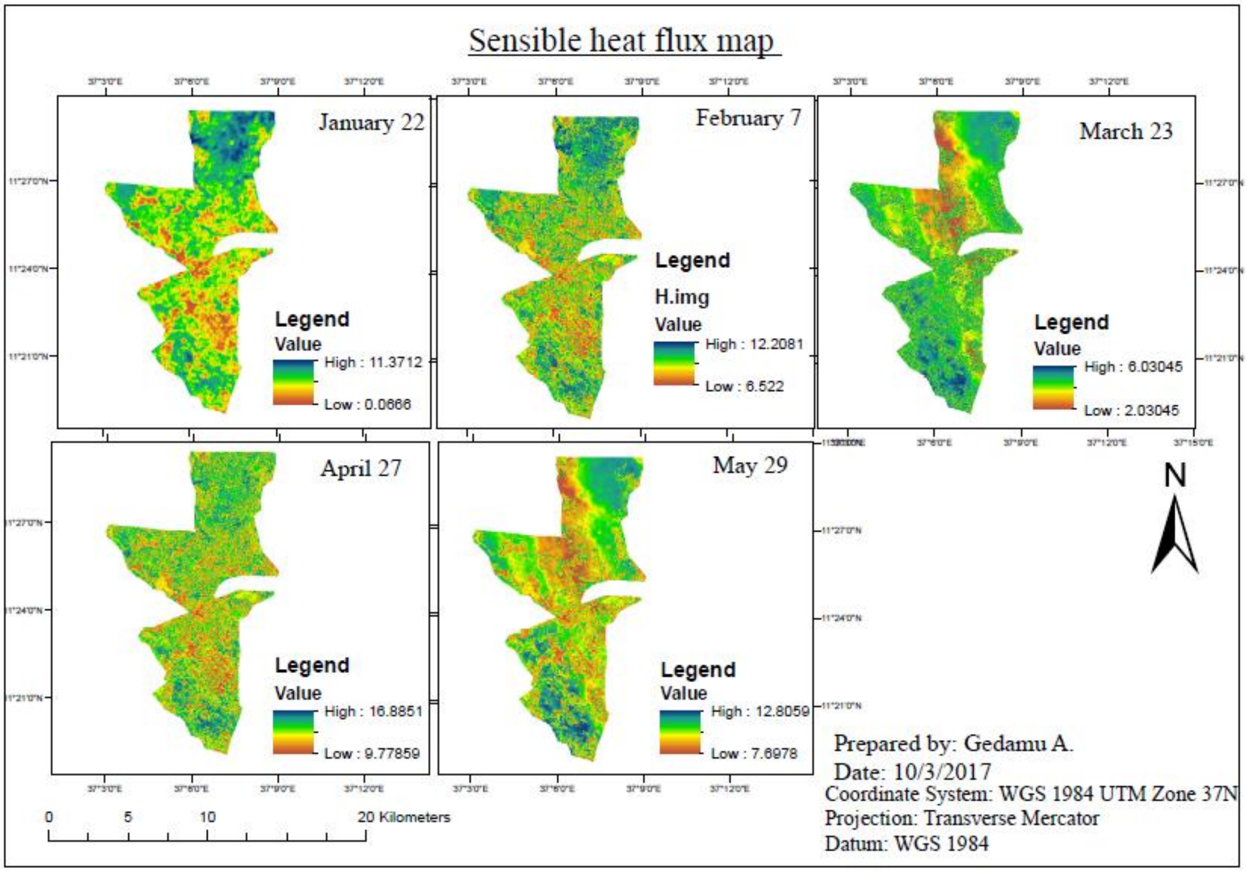

.